buildings

MDPI

Article

Field Tests and the Numerical Analysis of a Pile-Net Composite Foundation for an Intelligent Connected Motor-Racing Circuit

Xiaonan Wang [1,2] and Qitao Pei [2,*]

[1] Wuhan Urban Construction Investment Development Group Co., Ltd., Wuhan 430023, China; xnwang1975@126.com
[2] Wuhan Municipal Engineering Design & Research Institute Co., Ltd., Wuhan 430023, China
* Correspondence: pqt011@163.com

Abstract: In response to the problem of significant post-construction settlement that may occur in a motor racing circuit (MRC), two representative composite foundation testing areas, PHC pile (pre-tensioned spun high-strength concrete pile) and CFG pile (cement fly ash gravel pile), were selected for field tests to obtain the deformation law of pile–soil. Then, finite element numerical simulation was used to carry out back analysis on the geological mechanical parameters of the testing areas. The results showed that the error of soil settlement between the piles in the PHC pile and CFG pile testing areas were 8.2% and 9.6%, respectively, with good inversion precision. The obtained geological mechanical parameters can be used to predict the settlement of the rest of the MRC. On this basis, a finite element numerical model was constructed to analyze the bearing and deformation characteristics of the foundation of the MRC under five types of working conditions that may cause significant post-construction settlement. It showed that the settlement of the embankment was large in the middle and small on both sides after the consolidation of the embankment. The maximum settlement was about 27.0 mm, and the maximum longitudinal uneven settlement ratio of the embankment was 1.3/4000. The axial force of piles in the PHC pile and CFG pile composite foundations increased first and then decreased with depth. The maximum bending moment was located at the foot of slopes or at the boundary of strata, which was relatively small in the middle of the embankment. The deformation of the embankment and the bearing capacity of the piles could meet engineering requirements. This study has certain guiding significance for the design and construction of similar pile-net composite foundations.

Keywords: pile-net composite foundation; field test; soft soil; back analysis; numerical analysis

Citation: Wang, X.; Pei, Q. Field Tests and the Numerical Analysis of a Pile-Net Composite Foundation for an Intelligent Connected Motor-Racing Circuit. *Buildings* **2024**, *14*, 174. https://doi.org/10.3390/buildings14010174

Academic Editors: Eugeniusz Koda, Yong Tan and Suraparb Keawsawasvong

Received: 17 October 2023
Revised: 30 December 2023
Accepted: 8 January 2024
Published: 10 January 2024

1. Introduction

A large number of deep soft clay layers are distributed in the southeastern coastal areas of China, the Yangtze River Basin, and other areas. Soft clay has the characteristics of low shear strength, strong compressibility, and high water content, and has poor engineering properties [1,2]. Building roads in these areas without the proper treatment of the roadbed can easily cause the problems of embankment instability, post-construction settlement, and differential settlement, seriously affecting the safety and comfort of the road's operation [3,4].

In recent decades, pile-net composite foundations have been widely used in the soft soil foundations of multiple projects (such as highways, railways, etc.) to improve the bearing capacity and stability of embankments, and reduce embankment settlement [5–8]. The composite foundation is composed of three parts: a reinforced cushion layer (geosynthetic materials and crushed stones), pile foundations, and soil between the piles. The key to the technology is to coordinate the pile soil load sharing ratio by laying a reinforced cushion layer in order to jointly bear the upper load and also create a good constraint effect on the lateral displacement near the slope foot [9]. However, the bearing mechanism of the upper embankment full of pile-net composite foundation is relatively complex, and it is

necessary to comprehensively consider the soil arching effect [10,11], tensile membrane effect [12], and deformation coordination between the embankment, geogrid, and the composite foundation.

In order to better apply pile-net composite foundation technology to practical engineering, domestic and foreign scholars have made a lot of achievements in the last 20 years. In terms of laboratory model tests, Hewlett and Randolph [13] studied the spatial distribution characteristics of the soil arch in filling soil above the pile cap based on the assumption of the ultimate state of soil stress. By using the concrete piles to support embankments, Chen et al. [14] found that the stress concentration ratio between the piles and soil in composite foundations varied with the relative displacement of the piles and soil, ranging from 3.0 to 10.0. Castro and Sagaseta [15] concluded that the stress concentration ratio is equal to the elastic modulus ratio of the column to the soil without considering the lateral deformation of the soil. Liu and Zhang [16] analyzed the pile–soil interaction, the lateral deformation, and settlement characteristics of pile-net composite foundations in sloped soft soil via centrifugal tests. Some other scholars have conducted in-depth analyses on the load transfer in pile–soil interactions by using different physical model testing methods [17–20], believing that the load transfer mechanism can be determined by the soil arching effect in the embankment filling and the membrane effect imposed by the geogrid plate and crushed stones.

In terms of field testing, Liu et al. [21] studied the performance of PCP piles (prestressed concrete pipe piles) based on 10,333 tests on the aspects of the length and slenderness ratio, the bearing capacity and length as well as diameter, and controlled factors affecting pile top settlement. Young et al. [22] regarded the mechanism of the rigid pile-net composite foundation as an organic combination of the soil arching effect, grid tension, and pile–soil sharing effects, and proposed that the optimal pile spacing is three times the pile diameter. Zhang et al. [23] believed that the necessary condition for the occurrence of the soil arching effect is the differential settlement between the piles and soil. The modulus of the foundation soil decreases exponentially with the increase of settlement, and the variation range of the pile–soil load sharing ratio is 0.24–0.71. Yang and Liu [24] studied the settlement deformation of embankments, pore pressure dissipation, and pile–soil pressure distributions under a pile-net composite foundation.

In terms of numerical simulation, Zhang et al. [25] and Zhang et al. [26] analyzed the effect of sensitive factors such as the pile modulus, pile diameter, and cushion thickness on embankment settlement. Yoo [27] and Zhao et al. [28] studied the values of crushed stone and grid materials, and found that the modulus of crushed stone can be taken as 25 MPa in three-dimensional numerical calculations, and that the axial tensile stiffness of grid materials is 1000~4000 kN/m. Some scholars also consider the M-C model to be a more commonly used model with wider practicability [29], whereas the modified Cam-clay (MCC) model is usually used for soil simulation close to normal consolidated clay [30]. It is well known that the selection of constitutive model parameters has a great influence on the calculation results. Since the MCC model overestimates the peak friction angle of consolidated soil due to its elliptical yield surface [31], the prediction accuracy of its model is also affected by many factors (such as particle size, weathering degree, saturation, and the over-consolidation rate (OCR), etc.) [32,33], and the superposition of these factors may lead to the inaccuracy of the calculation results of the model. With the use of more advanced models, the number of parameters to be determined increases, which makes these models complicated to use, and a lack of knowledge of these parameters may result in inaccuracy in the obtained results. Therefore, enhancing the identification and rational application of constitutive model parameters is an effective way to improve the accuracy of numerical calculation.

In terms of theory, Kousik [34] and Zhuang and Wang [35] systematically studied the mechanism of the soil arching effect under a pile–soil composite foundation. Zhao et al. [36] derived the PSSR equation from the combined influence of the soil arching effect, tension membrane effect, and pile–soil interaction. Chen et al. [37] analyzed the settlement and

negative friction of pile-net composite foundations based on one-dimensional nonlinear consolidation theory and a hyperbolic load transfer model. Yu et al. [38] proposed a general solution for the consolidation of composite foundations with concrete-cored sand gravel (CCSG) piles based on the assumption of equal strain. FILZ et al. [39] calculated the maximum displacement difference between piles and soil in typical unit bodies, and established deformation coordination equations in embankments, grids, and foundation soil. Luo and Lu [40] derived analytical formulas for the settlement deformation and pile–soil stress ratio of rigid pile composite foundations based on the differential equation of pile–soil load transfer.

The above scholars have mainly focused on the load transfer mode, pile–soil stress ratio, embankment load bearing, and deformation characteristics of pile-net composite foundations in homogeneous strata. However, there is little research on the bearing capacity and deformation characteristics of embankments under different transition zones of a pile-net composite foundation and multi-soil stratum with uneven distribution. Also, there is relatively sufficient research on pile-net composite foundations in fields such as highways, railways, airports, and housing construction, while there are few research results in deep soft soil areas such as motor racing circuits in ultra-high speed environments. In addition, the embankment settlement of motor racing circuits has a significant impact on traffic safety. On the one hand, the uneven settlement of embankments can lead to road deformation, uneven road surfaces, and unstable vehicle driving, thereby increasing the incidence of traffic accidents. On the other hand, embankment settlement leads to terrain deformation, affecting the road structure and posing a great threat to driving comfort and safety. Therefore, it is necessary to adopt stricter standards for controlling embankment settlement and deformation to ensure traffic safety. Considering that a motor racing circuit has the characteristics of high speed traffic (300 km/h or above), a long route (several kilometers long), strict settlement control requirements, and the risk of uneven settlement and foundation slip after filling and loading in deep soft soil areas, there is currently a lack of engineering experience to reference under similar complex conditions and with a high standard of control. It can be seen that the treatment of the soft soil foundation in this project is extremely difficult, which poses great challenges to the safe construction and subsequent normal operation of the project. So, this paper took the Wuhan intelligent connected motor racing circuit as its setting, and conducted a pile-net composite foundation treatment and quantitative analysis on the areas where there might be significant post-construction settlement and settlement difference in the engineering area, such as deep soft soil sections, sudden geological changes, and transition sections with different pile types. On this basis, the rationality of the soft soil foundation treatment scheme was comprehensively evaluated. The research results and engineering practice indicate that the comprehensive treatment design scheme for the pile-net composite foundation is reasonable and feasible. While meeting the requirements of economic and rapid construction, it provides a guarantee of the safe construction of the motor racing circuit and also provides reference for the treatment of similar deep soft soil foundations.

2. Project Overview

2.1. Project Introduction

The Wuhan intelligent connected motor racing circuit is located on the bank of the Dongjing River in Wuhan city, Hubei Province, China, with an area of approximately 875,000 square meters. The circuit is the only F2 class track in the world that is combined with a closed T5 class testing field. The position of the motor racing circuit is shown in Figure 1.

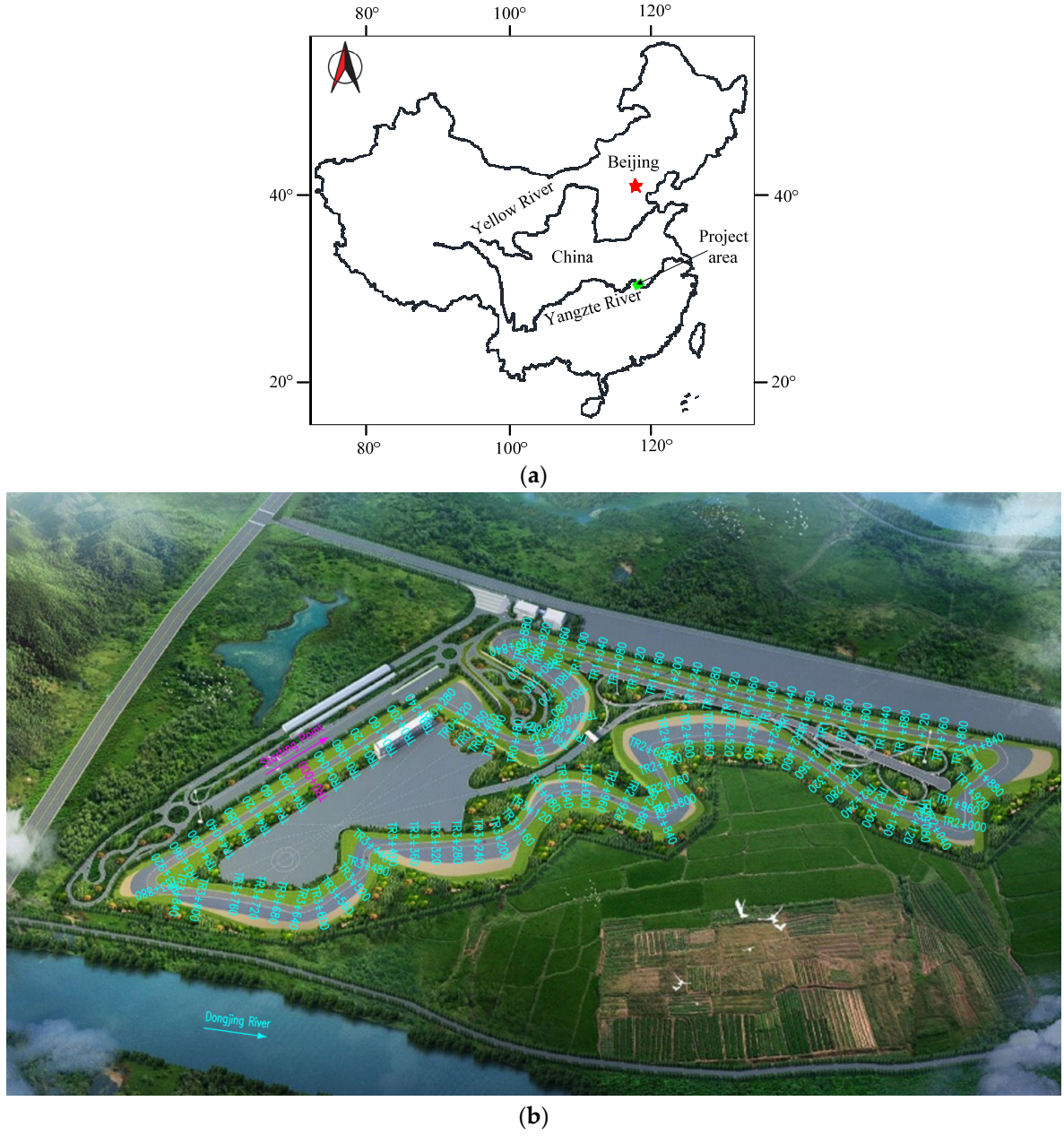

(**a**)

(**b**)

Figure 1. Project background, (**a**) regional map of the project in China. (**b**) Rendering of Wuhan International Circuit.

The main track of the motor racing circuit is a closed curve in a clockwise direction, with a mileage of K0 + 000~K4 + 237.21. The road has a total length of approximately 4.29 km, a width of approximately 50~190 m, and a speed limit of up to 300 km/h. The motor racing circuit is mainly used for high-speed control tests, high-speed network signal tests, and line-of-sight tests, etc., while also taking into account the performance competition of intelligent connected motor racing. Therefore, the tolerated settlement of the embankment in this project is relatively strict, with the post-construction settlement not exceeding 50 mm, and the longitudinal uneven settlement ratio of the embankment not exceeding 3/4000.

2.2. Geological Conditions

The racing track of this project mainly consists of ponds and ditches, with a small amount of wasteland distributed throughout. The shallow soil is pond mud, silt, cultivated

soil, miscellaneous fill, etc., with an uneven distribution of soil quality. The site is located on the first terrace of the Yangtze River, belonging to the geomorphic unit of the river accumulation plain.

Within the depth range of this survey, the distribution and engineering geological characteristics of the main strata in the project are as follows: The 1-1 plain fill, mainly composed of plastic silty clay, is located on the shallow surface, with a layer thickness of 0.20–4.2 m. The 1-2 silt is in a flow plastic state, with a thickness of 0.7–4.5 m. The 2-1 clay is mainly in a plastic state, with a thickness of 0.4–4.8 m. The 2-2 silty clay is mainly in a soft-flow plastic state, with a thickness of 1.0–10.9 m. The 2a clay is mainly in a plastic state, with a thickness of 0.7–4.7 m. The 2b silt is in a moderately dense state, with a thickness of 0.6–5.4 m. The 2-3 clay is in a plastic to hard plastic state, with a thickness of 0.9–7.5 m. The 4 silty clay is mainly in a soft plastic state, with a thickness of 0.4–14.3 m. The 4b silt is in a moderately dense state, with a thickness of 0.5–9.2 m. The 5-1 silty clay is mainly in a plastic state, with local areas in a soft plastic state, with a thickness of 0.4–7.4 m. The 5-2 clay is in a plastic to hard plastic state, with a thickness of 0.6–7.3 m. The 5-3 clay is in a plastic to hard plastic state, with a thickness of 0.9–8.0 m. The 5-4 silicon clay is in a plastic to hard plastic state, with a thickness of 0.5–2.9 m. The 6-1 silt is in a moderately dense state, with a thickness of 0.2–15.0 m. The 6-2 silty sand is in a moderately dense state, with a thickness of 0.1–17.5 m.

The groundwater at the site mainly consists of upper stagnant water and pore-confined water. The upper stagnant water mainly exists in the pores of the first layer of topsoil. The water level is buried at a depth of 0~2.60 m and has an elevation of 19.27~22.18 m. Pore-confined water mainly exists in the three sandy soil layers, which are closely related to the hydraulic system of the Yangtze River. Due to the upper cohesive soil and muddy soil being relatively impermeable layers, there is basically no hydraulic connection between the confined water at the site and surface water, and its impact on the project will be negligible.

2.3. Foundation Treatment Method

To avoid the differential settlement caused by the filling of new and old embankments at the junction of ponds, ditches, and other areas, the area was excavated to a depth of 19.5 m before undergoing deep foundation treatment. The site was divided into a low filling area, medium filling area, and high filling area according to the height of the embankment filling. The low filling area, with a filling height less than 3.0 m, was treated with the CFG pile composite foundation. For medium or high filling areas greater than 3.0 m, the PHC pipe pile composite foundation treatment was adopted. The distribution of foundation treatment methods for the racing track is shown in Figure 2.

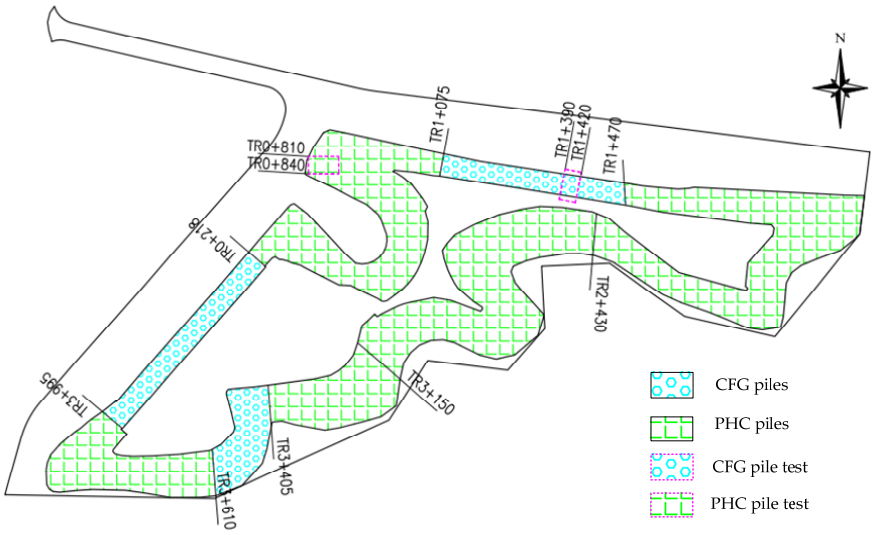

Figure 2. Schematic diagram of the embankment treatment methods for the racing track.

2.3.1. PHC Pile-Net Composite Foundation Treatment

The medium or high filling areas of the embankment were treated with a PHC pile-net composite foundation, as shown in Figure 3. According to geological conditions, the PHC pile has a wall thickness of 100 mm, arranged in a square with a pile spacing of 3.0 m. Also, it has a square pile cap of 1.5 m × 1.5 m × 0.35 m at the top, cast in place with C30 (compressive strength of 30 MPa) concrete. The top of the pile cap is laid with a 20 cm thick layer of crushed stone. After compaction, a number of steel and plastic geogrids (geogrids are laid at 20 cm intervals to the top of the embankment) are laid, and then filled with cement-stabilized soil and foamed light soil. The height of foamed light soil is determined according to the overall height of the embankment to ensure that the load at the top of pile is within the range of the target load. The length of a PHC pile is 15~25 m, and the designed characteristic value of a single pile's bearing capacity is 750~1100 kN.

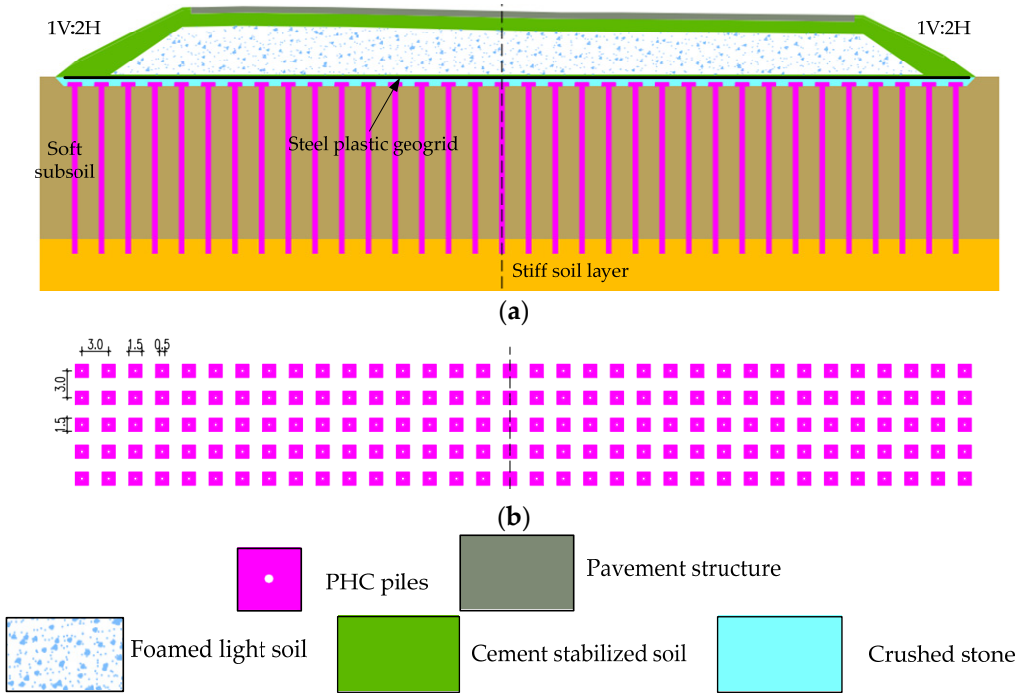

Figure 3. Treatment diagram of PHC pile-net composite foundation: (**a**) Cross section. (**b**) Pile location layout.

The PHC pile adopts the hammering method for pile sinking, and pile driving is carried out from the centerline of the track towards both sides. Before construction, the water in the pond should be drained. The silt at the bottom of the pond is removed down to 19.5 m, and a 40 cm layer of medium-coarse sand should be laid. After compaction, a 35 cm layer of graded crushed stone should be laid and compacted. Then, PHC pile construction can be carried out. Once the PHC pile is completed, the pile cap construction will be carried out, after excavation to 19.45 m.

In addition, before large-scale construction, PHC pile tests should be conducted on no less than three piles in each area. After 28 days of pile construction, the ultimate bearing capacity of a single pile can be determined by a static load test. The quality of the composite foundation should be mainly controlled by pile length, and the final penetration should not be less than 30 mm/10 blows.

2.3.2. CFG Pile-Net Composite Foundation Treatment

The low filling area of the embankment was treated with a CFG pile-net composite foundation, as shown in Figure 4. The CFG pile diameter is 0.5 m, arranged in a square with a pile spacing of 2.0 m. It has a square pile cap of 1.0 m × 1.0 m × 0.30 m at the top, cast in place with C30 concrete. The pile body is embedded 5 cm into the pile cap. A 20 cm

thick layer of crushed stone is laid on the top surface of the pile cap. After compaction, a steel/plastic geogrid is laid (a geogrid is laid every 20 cm to the top of the embankment), and then filled with cement-stabilized soil. The height of the cement-stabilized soil is determined based on the overall height of the embankment, ensuring that the load on the pile top is within the range of the target load. The length of a CFG pile is 16 m~18 m, and the characteristic value of a single pile's bearing capacity is not less than 300 kN. The characteristic value of the composite foundation's bearing capacity is not less than 160 kPa, and the pile body's strength should reach C20 (compressive strength of 20 MPa), while the pile cap's strength should be C30.

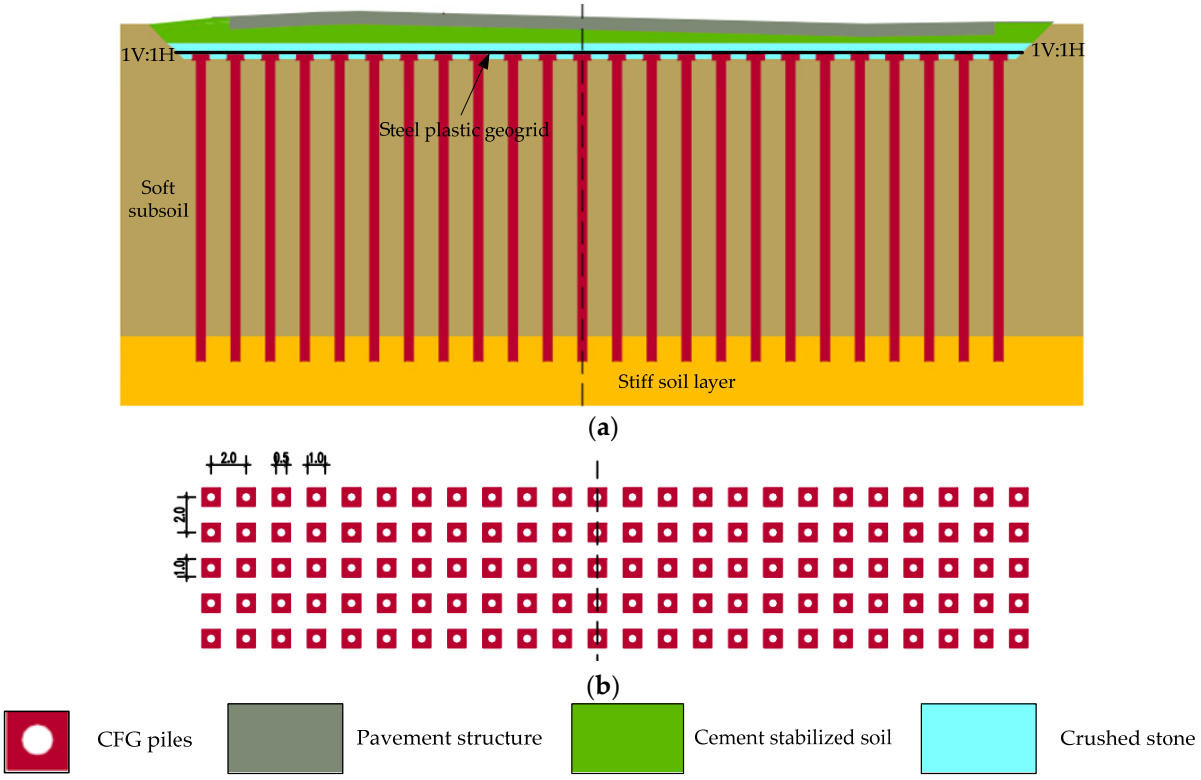

Figure 4. Treatment diagram of CFG pile-net composite foundation: (**a**) Cross section. (**b**) Pile location layout.

Before construction, unfavorable soil should be treated to a depth of 19.45 m, and then a 35 cm layer of graded crushed stone will be paved and compacted. Then, CFG pile construction can be carried out, and the pile's top elevation will be 19.5 m after excavation.

Similarly, before large-scale construction, CFG pile tests should be conducted on no less than three piles in each area. After 28 days of foundation pile construction, load tests should be used to determine the ultimate bearing capacity of a single pile and the ultimate bearing capacity of the composite foundation.

3. Field Tests

3.1. Test Sections

In order to obtain the pile–soil deformation characteristics of the pile-net composite foundation and provide a basis for the post-construction settlement prediction of the motor racing circuit, the Wuhan Institute of Rock and Soil Mechanics, Chinese Academy of Sciences, set up two representative test sections according to the thickness distribution difference of the soft soil and different pile types, as shown in Figure 2. In each test section, two monitoring cross sections were arranged, and the monitoring profiles of the different pile types are shown in Figures 5 and 6.

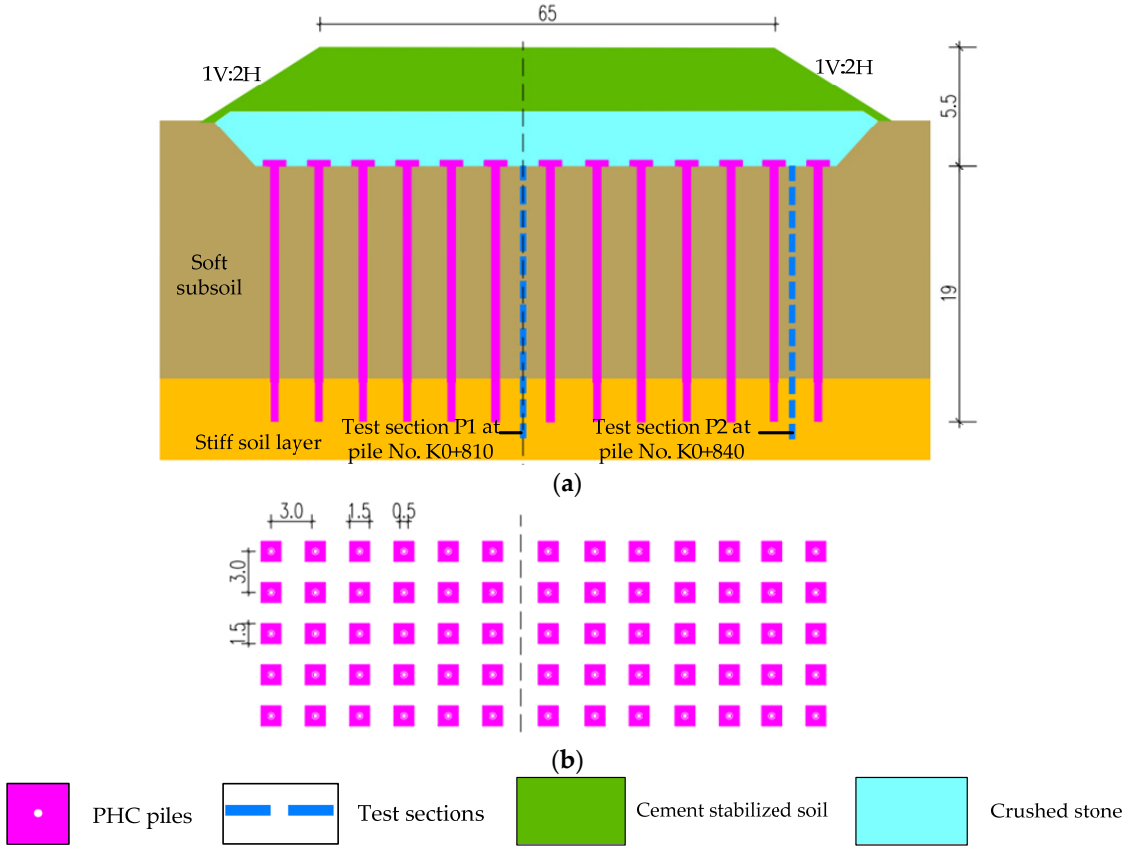

Figure 5. Loading schemes for PHC test: (**a**) Cross section. (**b**) Pile location layout.

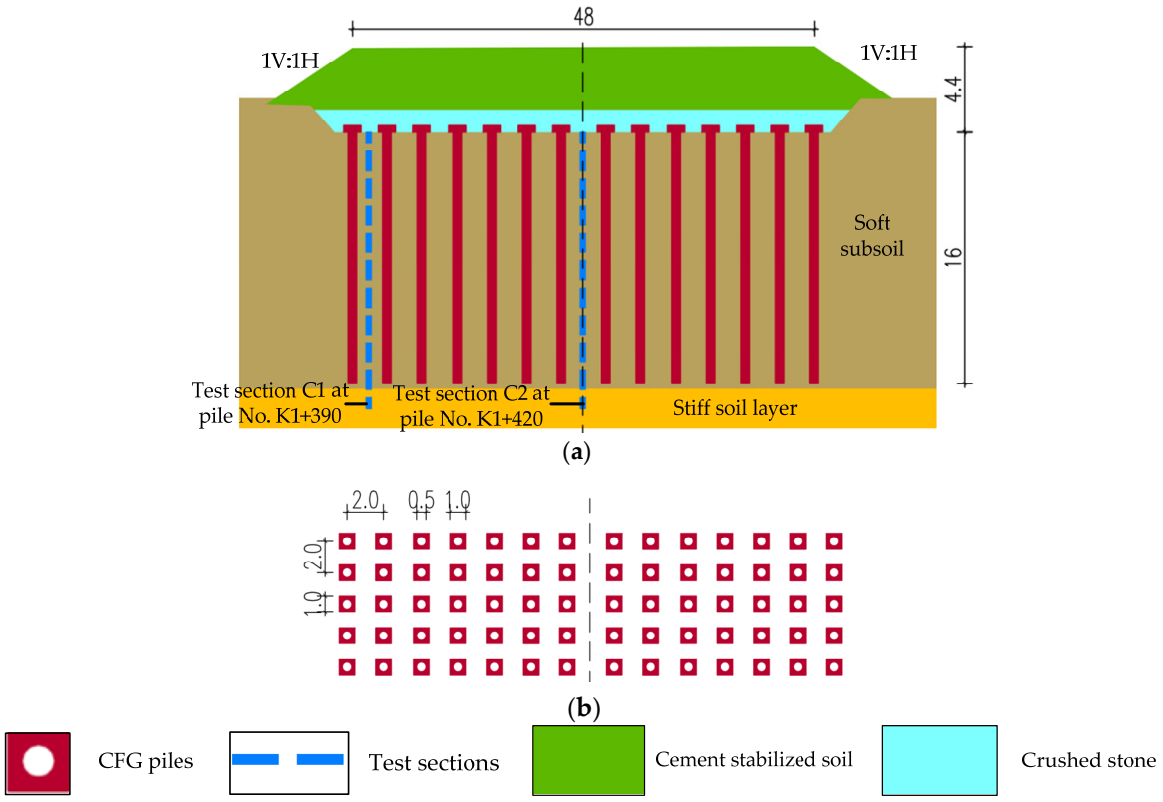

Figure 6. Loading schemes for CFG test: (**a**) Cross section. (**b**) Pile location layout.

(1) PHC test

Pile No. K0 + 810~K0 + 840 was treated with a PHC pile-net composite foundation with a length of 30 m and a width of 65 m. The P1 and P2 sections were located at the center and edge of the load, respectively. The distance between the P1 and P2 sections was 20 m.

(2) CFG test

Pile No. K1 + 390~K1 + 420 was subjected to a CFG pile composite foundation treatment with a length of 30 m and a width of 48 m. Similarly, the C1 and C2 sections were located at the edge and center of the load, respectively. The distance between the C1 and C2 sections was 20 m.

3.2. Layout of Monitoring Points

The settlement monitoring of this project is the key research content. The settlement of piles, settlement of soil between piles, peripheral settlement of the surcharge area, stratified settlement, surface horizontal displacement, deep horizontal displacement, pore water pressure, soil pressure monitoring, etc., should be tested. Since this section focuses on the monitoring of the settlement and deep horizontal displacement of pile tops and the soil between piles, the rest of the research is not discussed in detail, as recommended by study [41]. The monitoring sections are shown in Figures 5 and 6.

The settlement of the piles was observed by embedding settlement plates and test tubes at the pile head under the action of a pile load. Each test section selected five PHC piles or CFG piles, and there were a total of ten monitoring points, numbered ZT1~ZT10 (ZT stands for pile head). The monitoring points for the soil settlement between piles were arranged in the center of the pile group, designated as ZJ (ZJ stands for soil between piles), and there were ten monitoring points in total, numbered ZJ1~ZJ10. Deep horizontal displacement was observed via an inclinometer tube, and three deep horizontal displacement monitoring holes were arranged on the periphery of the monitoring section.

3.3. Test Scheme and Duration

After the test instrument has been checked, calibrated, and buried, the load test can be carried out. Based on the actual filling of the pile foundation, the actual load of the PHC and CFG pile-net composite foundations is 1.3 and 1.5 times that of the later working load of the pile foundation, respectively. Considering that the geogrid is easily damaged during construction, which affects the full performance of the reinforcement effect of the embankment, the geogrid material is taken as a safety reserve in the test and the subsequent analysis of the project, and its influence on the embankment is ignored. The loading profile of each test section is shown in Figures 5 and 6.

The project began in early December 2020 and finished in mid-December. Monitoring started after the full load was completed, and the monitoring was finished on 16 March 2021, lasting about 100 days. During the loading period and the 100 days after loading, there was no obvious soil collapse except for local small-scale soil collapses caused by continuous rainfall.

3.4. Test Results and Analysis

3.4.1. Settlement of the Pile Top and Soil between Piles

According to the measured data, the variation curves of typical section settlement over time under different pile tests are drawn, as shown in Figure 7. As can be seen from the figure, for the PHC pile-net composite foundation, the maximum settlement of pile head ZT3 was 13.6 mm, and the maximum settlement of soil ZJ4 between piles was 50.41 mm. The settlement of soil between the piles was 3.5~3.7 times that of adjacent pile heads. Similarly, for the CFG pile-net composite foundation, the maximum settlement of pile head ZT9 was 13.34 mm, and the maximum settlement of soil ZJ8 between piles was 39.65 mm. The settlement of soil between the piles was 2.7~3.0 times that of adjacent pile heads.

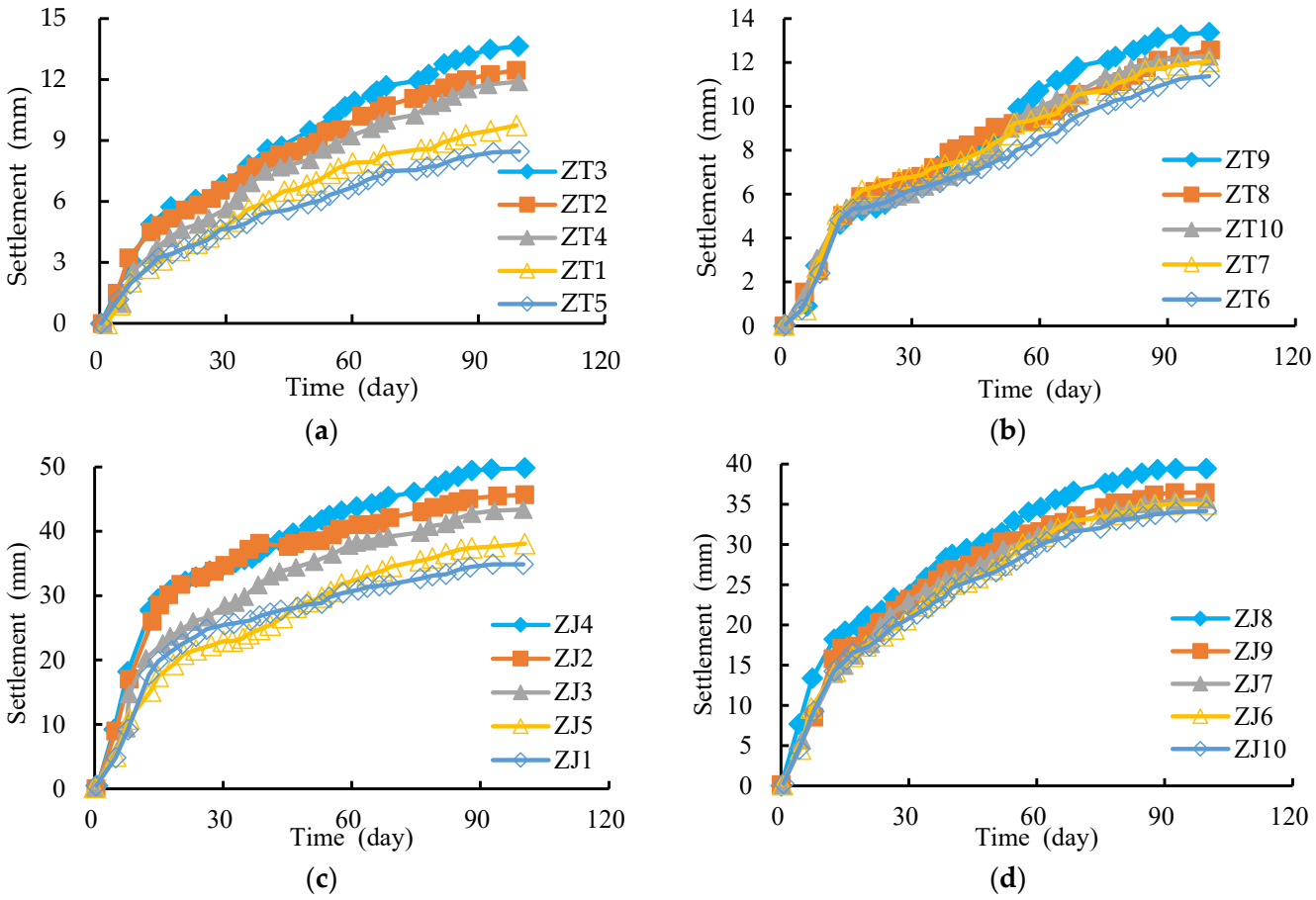

Figure 7. Relationship between soil cumulative settlement at the pile top or between piles and time under different pile tests: (**a**) Pile top of PHC test. (**b**) Pile top of CFG test. (**c**) Soil between piles of PHC test. (**d**) Soil between piles of CFG test.

Further analysis showed that in both the PHC pile and CFG pile composite foundation treatment areas, the settlement of the pile head and soil between the piles increased rapidly during loading, and decreased immediately after loading, but the cumulative settlement value still increased in a hyperbolic manner. By early March of 2021, the slope of the settlement–time curve began to decrease, that is, the settlement rate began to slow down.

3.4.2. Deep Horizontal Displacement

The deep horizontal displacement in the load area was monitored. Taking the test data at an interval of 20 days as the object, the variation curve of the horizontal displacement monitored by the inclinometer tube over time is shown in Figure 8. It can be seen from the figure that during the monitoring period, the lateral displacement of the soil in the load area did not exceed 1.5 mm, and the direction of lateral displacement was spread outward from the load center. On the whole, no obvious lateral compression deformation occurred in the soil of the PHC pile or CFG pile areas, and the lateral displacement gradually decreased with the increase of depth.

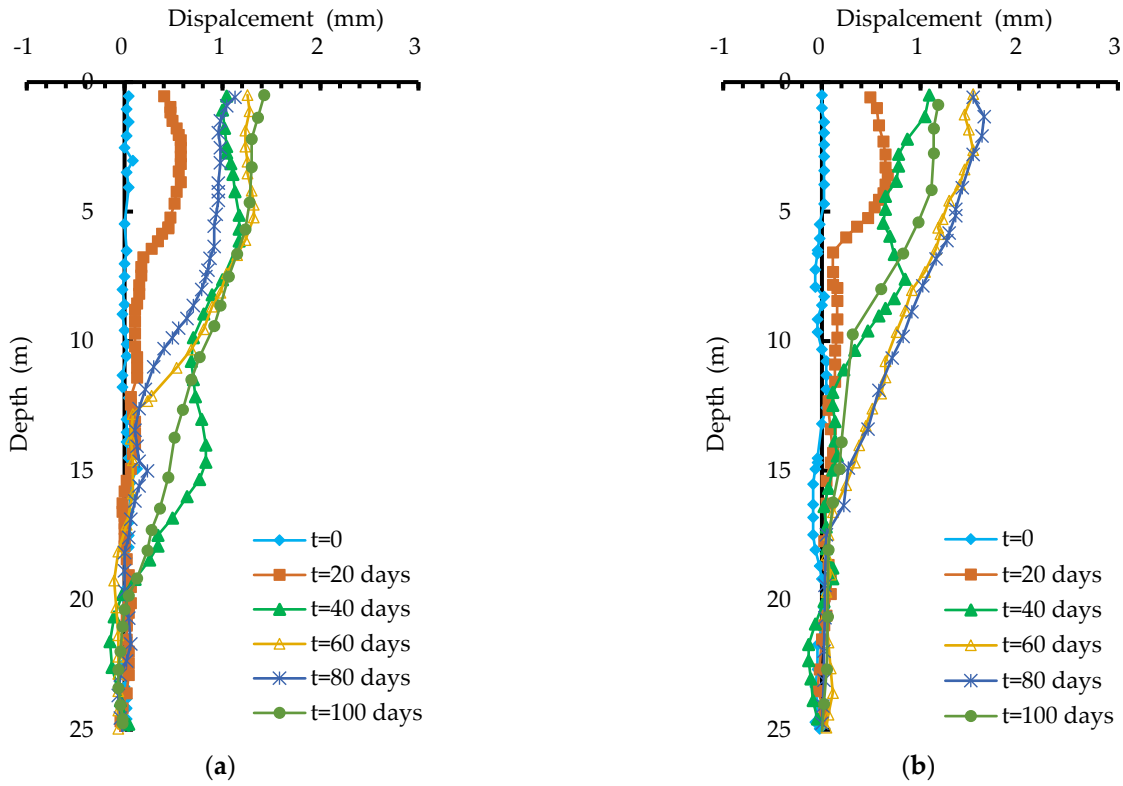

Figure 8. Curves of horizontal displacement of an inclinometer pipe with time under different pile tests: (**a**) PHC test. (**b**) CFG test.

4. Back Analysis of Stratum Parameters and the Reinforcement Treatment of Embankments

According to reference [41], the pile-net composite foundation in this test area generated a maximum excess pore water pressure of 80 kPa due to overloading, and the pore water pressure gradually dissipated with time. By early March 2021, there was still excess pore water pressure close to 20 kPa that had not yet dissipated. In theory, settlement may still have occurred during the test section, so it is necessary to predict the subsequent settlement.

4.1. The Numerical Model and Mesh Grids

The large commercial software 'MIDAS GTS NX 2022 R1 [42]' was used for the numerical simulation of this project. The calculation zones are located in sections of the PHC test and CFG test, and the numerical models are 100 m × 32 m (X × Y) and 100 m × 30 m (X × Y), respectively. The X-axis is parallel to the road axis and is positive along the road. The Y-axis extends from elevation −6.5 m to the top of the load. As shown in Figure 9, the grid model is set up based on topography, geological conditions, and loading materials, etc. Figure 9a shows the finite element model of the PHC pile-net composite foundation, which is divided into 13,005 grid elements and 13,831 nodes, respectively. Similarly, Figure 9b shows the calculation model of the CFG pile-net composite foundation, with a total of 11,628 grid elements and 13,108 nodes.

Considering the calculation range of the model and the arrangement of the pile body, the solid model in this paper is divided using quadrilateral grid elements. Through continuously adjusting the grid size (such as 1 m, 2 m, 3 m, 4 m, 5 m) and comparing the displacement calculation values with the measured ones, it was found that when the grid size of the soil strata, the piles, and pile cap are 2 m and 1 m, respectively, the calculation results are in good agreement with the measured values, and the calculation efficiency is optimal.

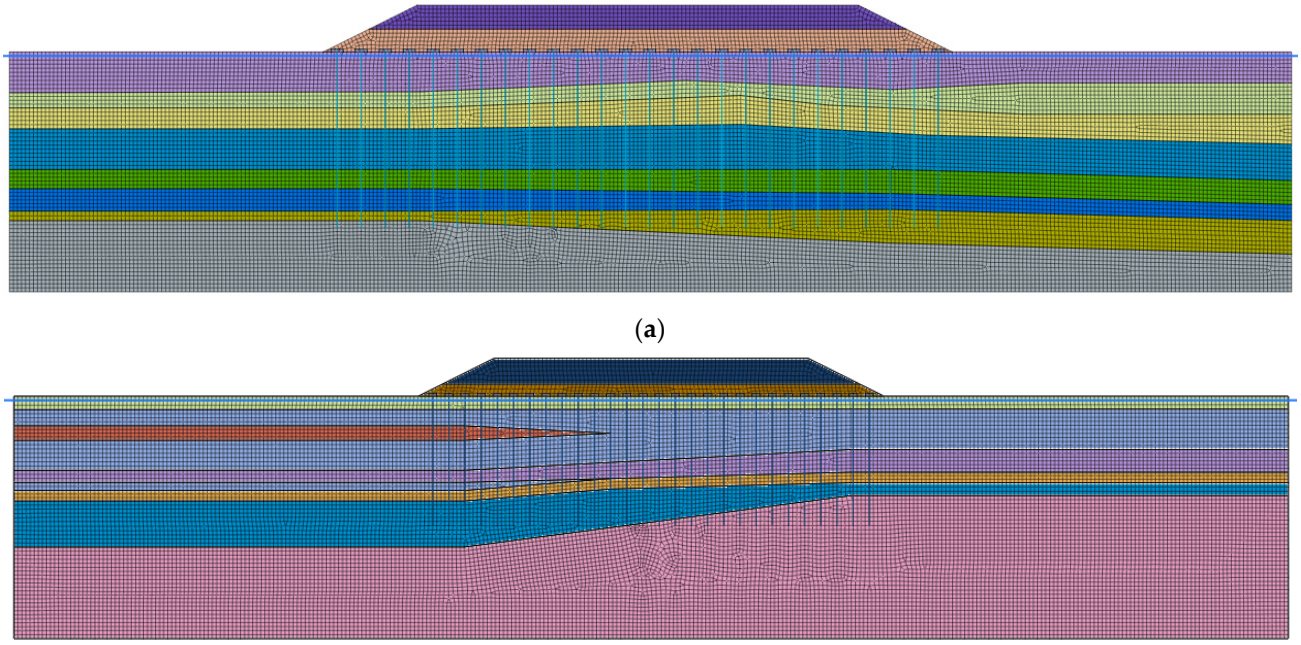

(**a**)

(**b**)

Figure 9. Finite element mesh model: (**a**) PHC pile-net composite foundation. (**b**) CFG pile-net composite foundation.

4.2. Constitutive Model and Computational Conditions

In the numerical calculation, the solid element is used to describe the behavior of the soil, crushed stone cushion, and embankment filling. The Mohr–Coulomb yield criterion is used for the constitutive model and soil consolidation is also considered. The elastic constitutive model is adopted for the pile cap, pile body, and pavement structure. The physical and mechanical parameters of the soil, loading materials, and pavement structure are shown in Tables 1 and 2, respectively. The structural parameters of the piles and their caps are shown in Table 3.

Table 1. Physical and mechanical parameters of the soil.

Category	Unit Weight /(kN/m^3)	Permeability Coefficient /(10^{-7}m/s)	Compression Modulus /MPa	Poisson's Ratio	Cohesion /kPa	Friction Angle /(°)
1-1 plain fill	19.9	1.0	5.3	0.3	12	10
1-2 silt	16.8	0.1	2	0.42	10	4
2-1 clay	19.5	0.2	5.2	0.32	18	10
2-2 silty clay	17.8	0.1	3	0.39	12	6
2-3 clay	19.9	0.2	7	0.4	22.8	12.4
2a clay	19.2	10	6.6	0.41	23	12
2b silt	19.5	0.6	5.7	0.35	15	21
4 silty clay	18.9	0.1	4.5	0.39	13.5	9.3
4b silt	19.6	50	8.5	0.35	14	23
5-1 silty clay	19.1	0.1	5.5	0.36	18.8	11
5-2 clay	19.2	0.2	7.5	0.38	26.5	13.2
5-3 clay	19.5	0.2	9.2	0.27	39.5	14.7
5-4 Silty clay	19.6	0.1	6.2	0.35	21	11
6-1 Silt	19.7	50	10	0.3	10	20
6-2 Silty sand	20	500	17	0.3	0	34

Table 2. Physical and mechanical parameters of loading materials and pavement structure.

Category	Unit Weight /(kN/m^3)	Elastic Modulus /MPa	Poisson's Ratio	Cohesion /kPa	Friction Angle /(°)
Crushed stone	22	50	0.25	0	30
Embankment filling	19	40	0.25	23	11
Pavement structure	25	3000	0.2	-	-

Table 3. Structural parameters of piles and their caps.

Category	Unit Weight /(kN/m^3)	Elastic Modulus /GPa	Poisson's Ratio	Normal Stiffness /(10^6 kN/m^3)	Shear Stiffness /(10^6 kN/m^3)
CFG pile	22	10~20	0.2	1~4.5	0.09~0.4
PHC pile	25	15~30	0.2	1.3~12	0.1~1.1
Pile caps	25	30	0.2	/	/

The normal displacement at the bottom of the model, as well as the horizontal displacement at the periphery of the model, are all constrained. The action of tectonic stress is ignored, only self-weight is considered.

4.3. Back Analysis of Stratum Parameters

The soil mechanical parameters mentioned above are obtained from laboratory tests, and the influence of pile construction and embankment filling disturbance has not been considered. In addition, the structure parameters of the piles are all empirical values. Therefore, it is necessary to invert the soil mechanical parameters and pile modulus in the project by combining the settlement monitoring data of the piles and soil between piles, so as to obtain more practical calculation parameters, considering construction disturbance.

The flow chart of the back analysis of soil and pile parameters is shown in Figure 10, mainly involving several aspects, which are considered using the following approaches:

(1) The selection of monitoring information on displacement. Prior to back analysis computation, proper monitoring information on displacement needs to be selected so as to obtain reasonable equivalent soil mechanical parameters and a pile modulus. In general, the selection should follow the following principles: (a) the monitoring information needs to be accurate and reliable without abnormal changes; (b) the monitoring information should be complete, information recorded by pre-buried monitoring equipment should be selected as a priority to carry out the back analysis of complete displacement; (c) the monitoring information needs to be adequate and representative; and (d) the monitoring information should change slightly and no invalid values should be used. Based on the above selection principles, the monitored data of soil settlement between piles at the two test sections (see Section 3.1) are selected. In this way, the monitoring points involved in the back analysis of the mechanical parameters of soil can be easily determined.

(2) Determination of inversion parameters. Soil strata at the test sections mainly include 2-2 silty clay, 2a clay, 4 silty clay, and 6-1 silt, and the parameters of the pile modulus have a significant impact on the embankment settlement. Namely, six parameters highly sensitive to embankment settlement are subjected to back analysis, including the deformation moduli of 2-2 silty clay, 2a clay, 4 silty clay, and 6-1 silt, and the elastic modulus of PHC piles and CFG piles. Therefore, in total six parameters need to undergo back analysis.

(3) The back analysis method. By optimizing the back propagation (BP) network structure through a genetic algorithm (GA), the GA-BP method can be formed [43]. This method has great advantages in its nonlinear mapping and global search ability, and has been widely applied in the back analysis of parameters. In order to obtain reasonable soil and pile parameters, the uniform design method and the GA-BP method are comprehensively used for parameters' inversion. First, the scope of the parameters

for back analysis were determined based on the results of field tests, laboratory experiments, and engineering experience. Then, the uniform design theory was used to design experiments through combinations of multiple parameters and levels, thus obtaining multiple groups of samples for orthogonal analysis. Afterwards, the above samples were imported into a neural network optimized by the genetic algorithm to perform network training and attain the nonlinear mapping relation between the parameters for back analysis and the monitored displacement. Finally, the measured values were input into the trained network to obtain the mechanical parameters for back analysis. According to calculation results from back analysis, the deformation moduli of 2-2 silty clay, 2a clay, 4 silty clay, and 6-1 silt within the disturbance range were 6.2 MPa, 13.2 MPa, 9.0 MPa, and 21.0 MPa. The elastic moduli of the PHC piles and CFG piles are 19.5 GPa and 12.0 GPa, respectively.

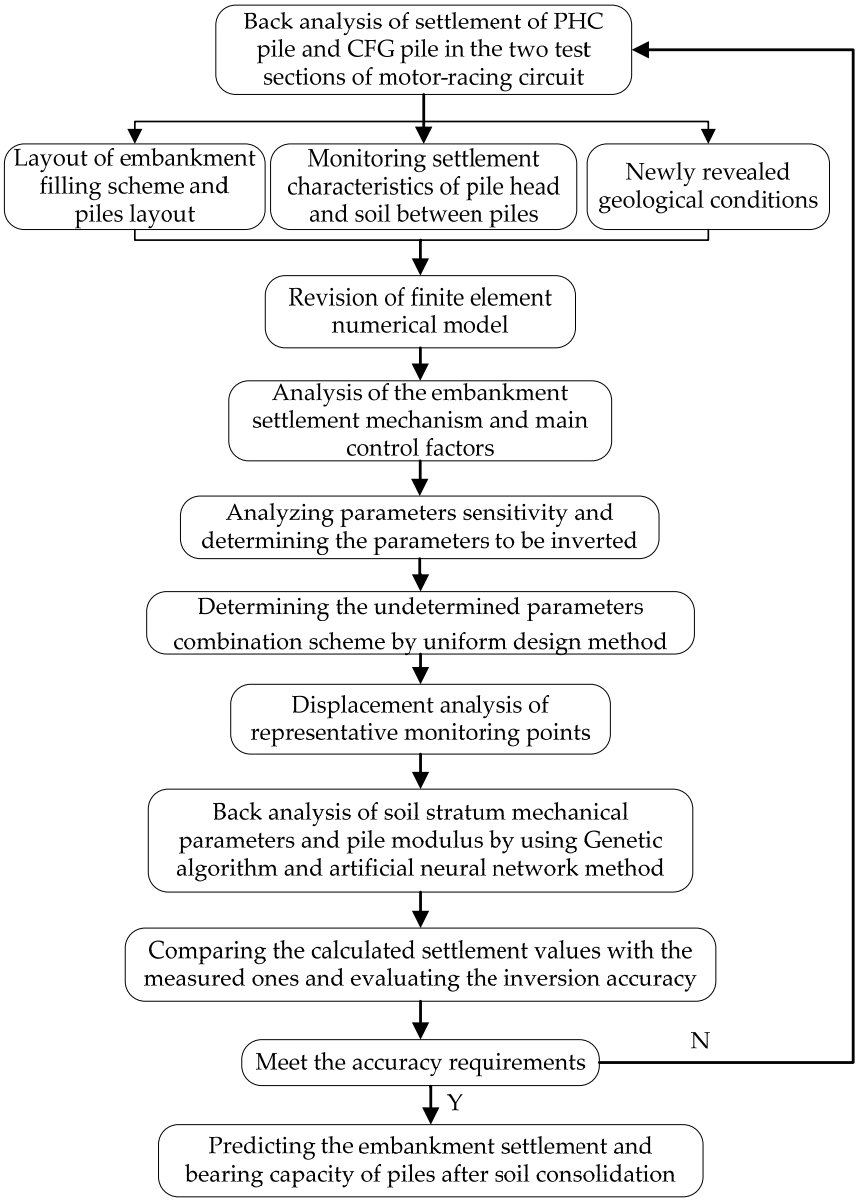

Figure 10. Schematic diagram of the back analysis of soil mechanical parameters and pile moduli.

4.4. Evaluation of the Results Using the Back Analysis Method

Figure 11 plots the comparison between the calculated and measured values of soil settlement between piles under different pile-net composite foundation treatments. Figure 12 shows the contour maps of settlement after soil consolidation under different pile-net

composite foundation treatments. It can be seen that the variation trend of the measured data and the calculated value are basically consistent. The results can be specifically listed as follows: (1) when the PHC pile test was finished, the measured maximum settlement of the soil between piles was 50.4 mm, and the calculation value via back analysis was 54.5 mm, with an error of 8.2%. After the soil consolidation was completed, the maximum settlement was 70 mm. (2) Similarly, once the CFG pile test was finished, the measured maximum settlement of the soil between the piles was 39.65 mm, and the calculation value was 43.4 mm, with an error of 9.6%. After soil consolidation was basically completed, the maximum settlement reached 59 mm. (3) Whether the PHC pile or CFG pile test, the calculation values from back analysis were slightly greater than the measured ones, and the maximum error did not exceed 10%, indicating that the inversion accuracy was good and could meet the engineering requirements.

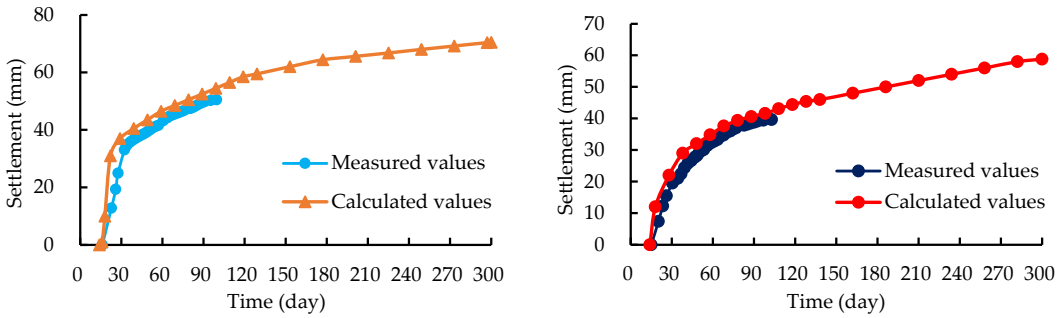

Figure 11. Comparison between the calculated and measured values of soil settlement between piles under different pile-net composite foundations: (**a**) PHC pile-net composite foundation. (**b**) CFG pile-net composite foundation.

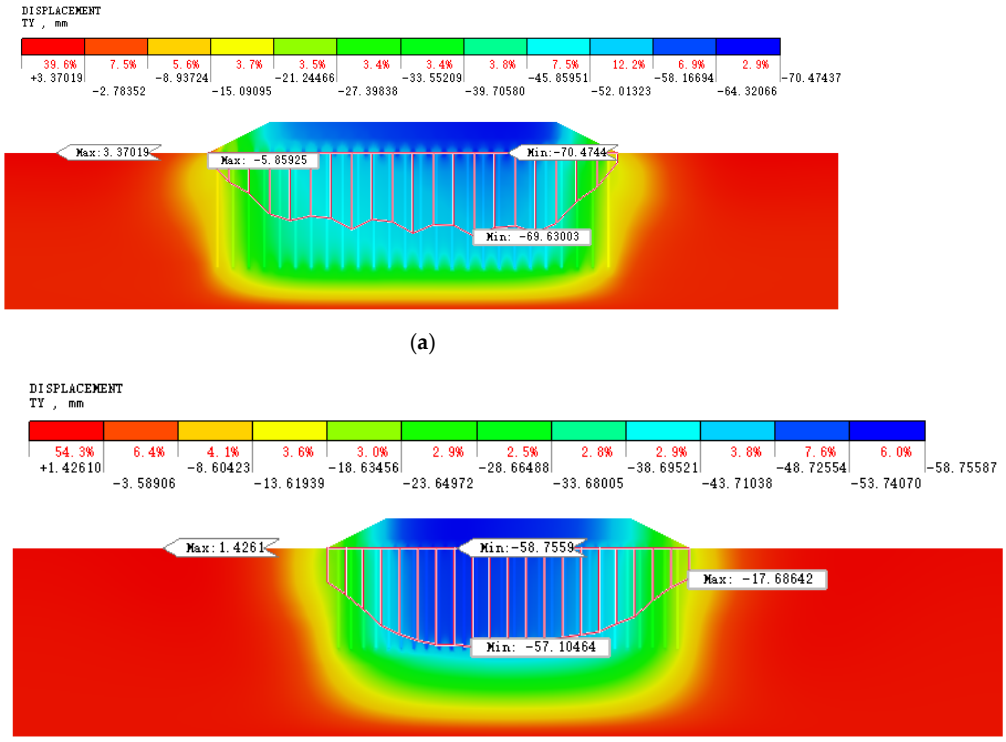

Figure 12. Contour maps of settlement after soil consolidation under different pile-net composite foundations: (**a**) PHC pile-net composite foundation. (**b**) CFG pile-net composite foundation.

However, due to the fact that after the field test there was still an excess pore water pressure of nearly 20 kPa that had not dissipated, there might still be settlement in the test sections, which was consistent with the trend of the calculation results. Furthermore, the maximum settlement of the soil between piles through the PHC and CFG pile-net composite foundation treatments could reach 70 mm and 59 mm, respectively, which were greater than the specified 50 mm settlement standard. Therefore, it is necessary to reinforce embankments in these areas.

4.5. Embankment Reinforcement Treatment and Its Effectiveness

4.5.1. Embankment Reinforcement Treatment

In the PHC pile test area, the bottom of the PHC pile has not entered the stable stratum, and the bearing capacity of the pile-net composite foundation is insufficient due to poor geological conditions. The cross-section of the PHC pile reinforcement is shown in Figure 13a. The layout of the pile positions in the reinforcement section is shown in Figure 13b. The reinforcement treatment methods are described as follows: (1) The driving of the PHC piles was repeated and penetration control adopted, that is, the final penetration should not be less than 30 mm/10 blows. (2) The soil between piles was reinforced by cement–soil mixing piles, which passed through 2-2 silty clay and 2a clay for about one meter.

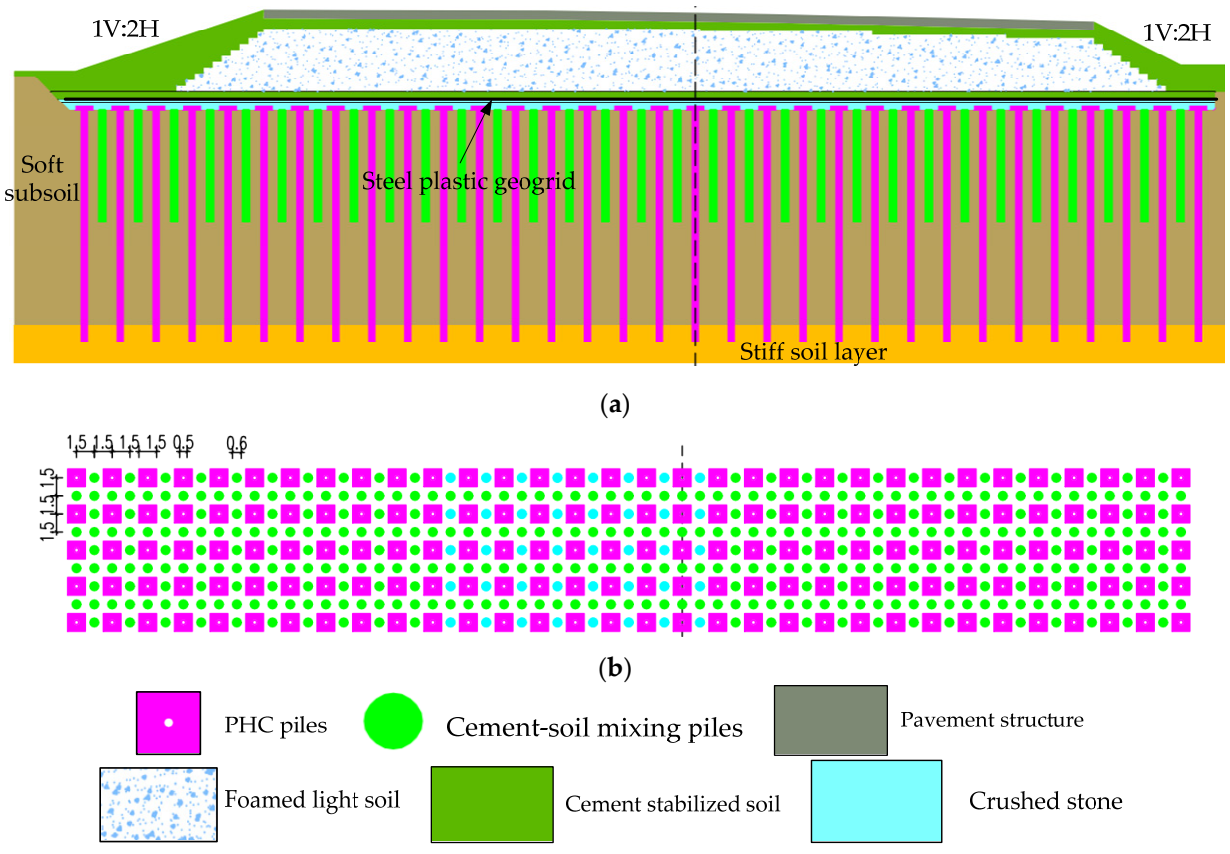

Figure 13. Reinforcement diagram of pile-net composite foundation embankment in the PHC test section: (**a**) Cross section. (**b**) Pile location layout.

Similarly, for the CFG pile test area, due to the poor geological conditions, the bearing capacity of the CFG pile-net composite foundation was insufficient. The cross-section of the CFG pile reinforcement is shown in Figure 14a. The layout of the pile positions in the reinforcement section is shown in Figure 14b. In order to improve the bearing capacity of the composite foundation, additional CFG piles need to be installed in these areas, and the pile bottom should penetrate the sand to about one meter.

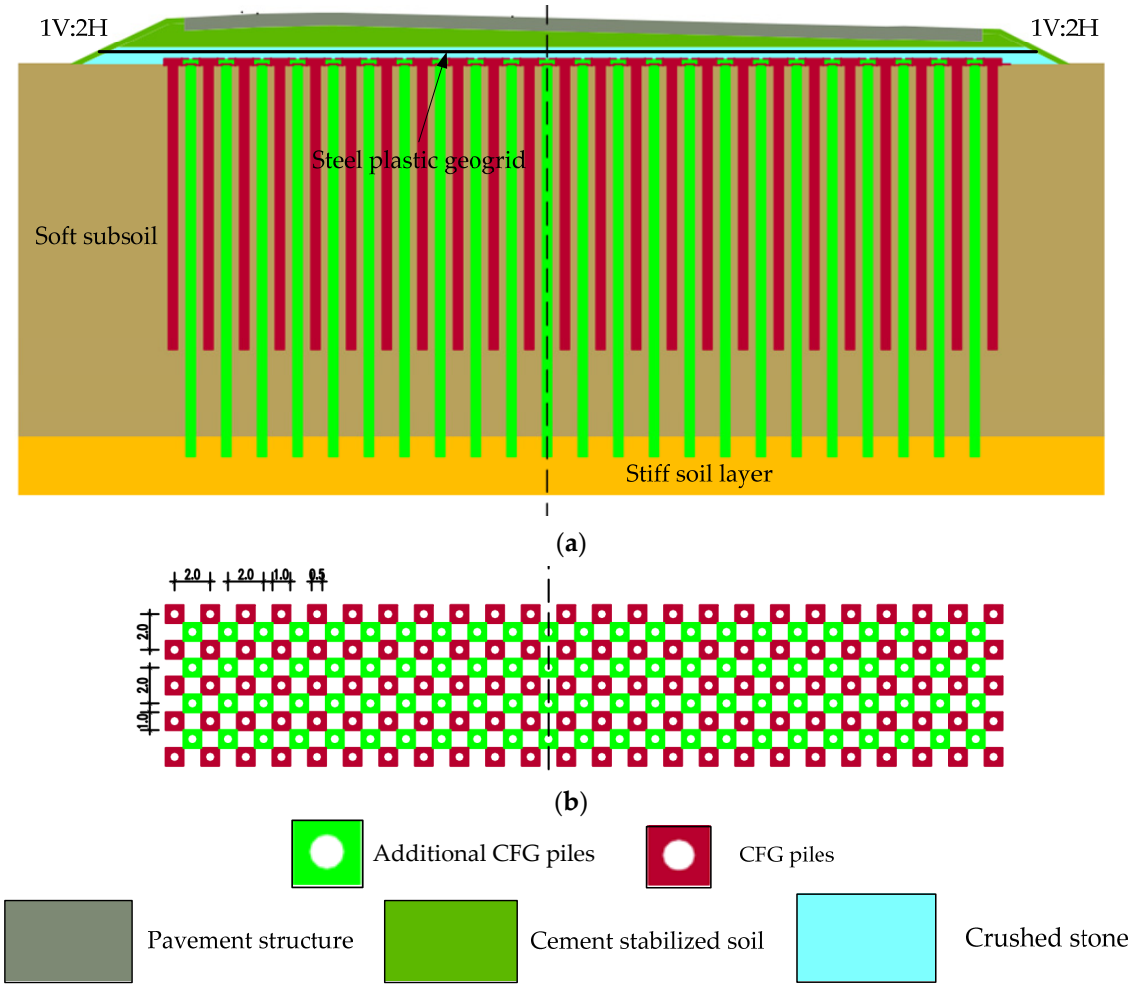

Figure 14. Reinforcement diagram of pile-net composite foundation embankment in CFG test section: (**a**) Cross section. (**b**) Pile location layout.

4.5.2. On Site Implementation Effect

In order to obtain the settlement after embankment reinforcement, four observation points of the pile top settlement and four observation points of the soil settlement between piles were set up in the PHC pile test area. In addition, in the CFG pile test area, two settlement observation points in the middle of the embankment and two monitoring points in the shoulder of embankment were also set up. By November 2021, the filling of the embankment had been completed, the pore water pressure had started to dissipate and the settlement was basically stable.

The cumulative settlement curve of each point after reinforcement in the PHC pile test area was shown in Figure 15a. As shown in the figure, after the completion of embankment construction, the cumulative minimum settlement point was ZD3, with a settlement value of 7.11 mm. The cumulative maximum settlement point was ZJ4, with a settlement value of 21.01 mm. Similarly, the cumulative settlement curve of each point in the CFG pile test area is shown in Figure 15b. It can be seen that after the completion of embankment construction, the cumulative minimum settlement point was LJ1, with a settlement value of 13.77 mm. The cumulative maximum settlement point was LZ2, with a settlement value of 15.88 mm. The cumulative settlement at each measuring point in the two test areas meets the design requirements.

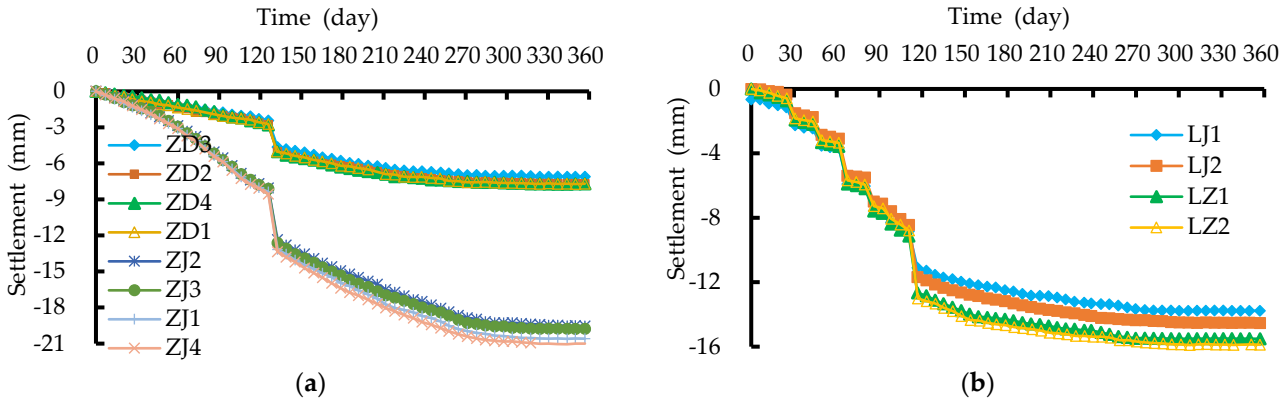

Figure 15. Accumulated settlement curves of the pile top and soil between piles after reinforcement in different pile test areas: (**a**) PHC pile test. (**b**) CFG pile test.

5. Numerical Simulation Analysis of the Typical Working Conditions of the Intelligent Connected Motor Racing Circuit

The motor racing circuit mainly adopted CFG pile and PHC pile-net composite foundations. In order to evaluate the differential settlement caused by different embankment treatment methods in the transitional area and the area where the settlement is likely to be large (such as sudden changes in the strata), five typical working conditions were selected for the finite element numerical simulation analysis based on geological conditions, pile-net size and layout, and embankment settlement standards. The specific working conditions and pile numbers were (1) Condition 1: the PHC pile area in the cross-section at pile number TR3 + 260; (2) Condition 2: the CFG pile area in the cross-section at pile number TR1 + 440; (3) Condition 3: the PHC pile area along the longitudinal section between pile number TR1 + 700 and TR1 + 800; (4) Condition 4: the CFG pile area along the longitudinal section between pile number TR3 + 460 and TR3 + 560; and (5) Condition 5: the PHC pile and CFG pile transition area between pile number TR0 + 160 and TR0 + 260. The typical working condition positions are shown in Figure 16.

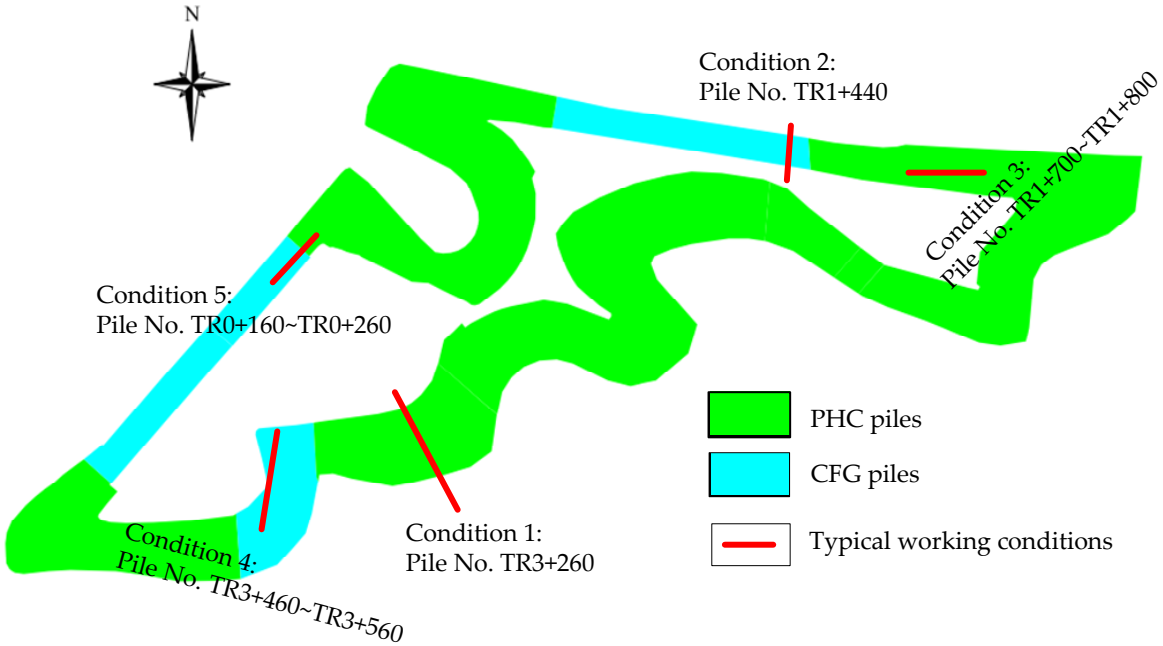

Figure 16. Typical working condition positions of the motor racing circuit.

5.1. Model Construction and Mesh Grids

Typical two-dimensional numerical models are established based on soil strata, embankment filling materials, pile caps, pile bodies, the pavement structure, etc. In order to reduce the influence of the boundary effect of the model on the calculation results, the width of the model should be 2~3 times the width of the embankment, and the depth of the model is should be as 1.5~2 times that of the pile length [44]. The Y-axis is positive along the elevation direction, and the X-axis is positive along the road pile number direction. The size of the numerical model is 100 m × 40 m (X × Y).

The finite element numerical models under typical working conditions are shown in Figure 17. Figure 17a,b plot the cross-sectional calculation models of the PHC pile-net composite foundation under Condition 1 and the CFG pile-net composite foundation under Condition 2, respectively. Figure 17c,d plot the longitudinal section calculation models of the PHC pile-net composite foundation under Condition 3 and the CFG pile-net composite foundation under Condition 4, respectively. Figure 17e plots the transition zone model of the PHC pile and CFG pile-net composite foundations under Condition 5.

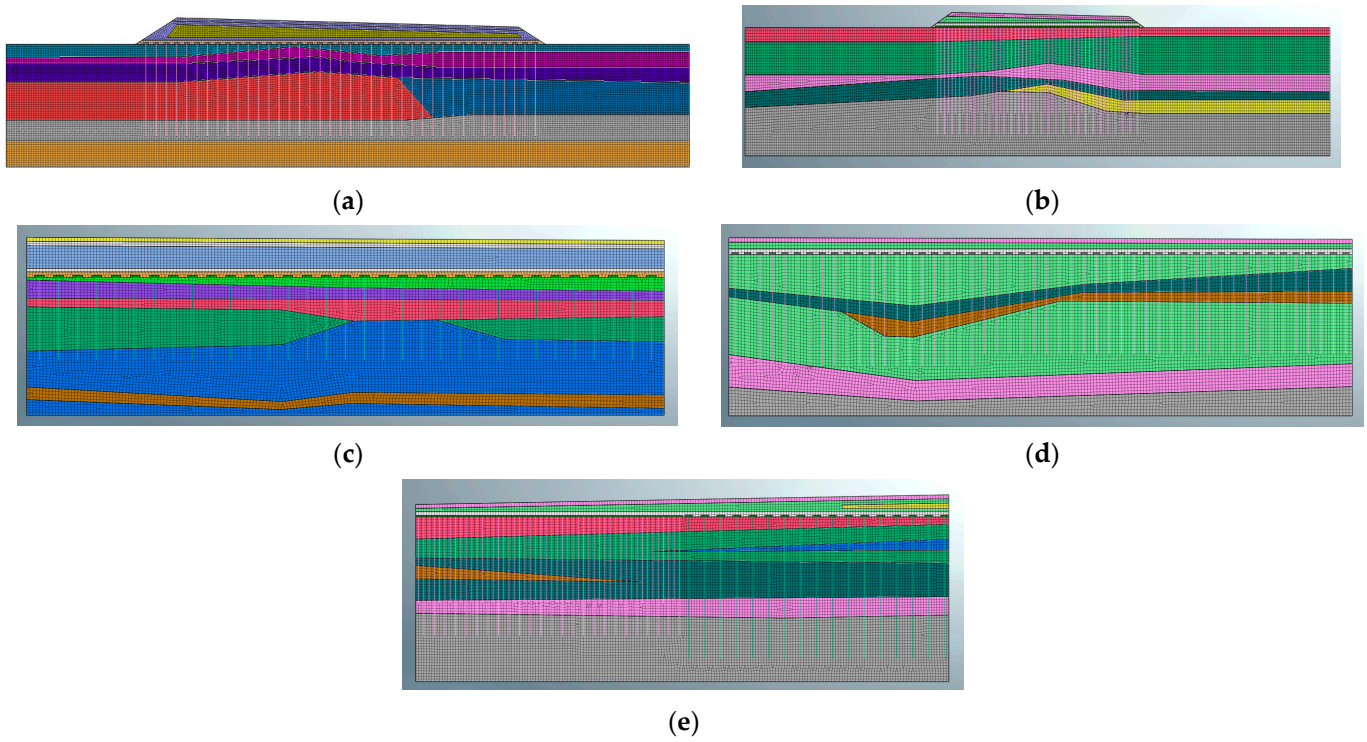

Figure 17. Calculation models under typical working conditions: (**a**) Condition 1. (**b**) Condition 2. (**c**) Condition 3. (**d**) Condition 4. (**e**) Condition 5.

5.2. The Constitutive Model and Calculation Conditions

Solid elements were used to simulate each soil stratum and embankment filling in the model, and the Mohr–Coulomb elasto-plastic criterion was adopted in the constitutive model. The elastic constitutive model was adopted for the pile cap, pile body, and pavement structure. Some soil stratum parameters, such as 2-2 silt clay, 2a clay, 4 silty clay, and 6-1 silt, as well as the elastic modulus of the PHC pile and CFG pile bodies, were obtained via back analysis (see Section 4.3). The other parameters were consistent with Section 4.2.

The bottom displacement of the model and the horizontal displacement on both sides of the model were constrained. The groundwater level in the model was set to one meter below the surface. Since the embankment was built in a soft soil stratum with a shallow groundwater level, the excess pore water pressure would suddenly increase and effective stress would decrease during the filling process, so the generation and dissipation of the excess pore water pressure should be considered. Consolidation analysis was adopted

here. The hydraulic boundary conditions were set as follows: both sides of the model were undrained boundaries, and the surface and bottom of the model were drained boundaries.

5.3. Analysis of Calculation Results

5.3.1. The Effect of the Pile-Net Composite Foundation on Settlement

Figure 18a,b show the settlement displacement contour maps of the pile-net composite foundation along the cross-section of the embankment under Condition 1 (PHC pile) and Condition 2 (CFG pile) at the end of soil consolidation, respectively. The figures also plot the surface settlement curves under different working conditions. It can be seen that within the range of the foot of the embankment, the settlement curve of the embankment approximately presents an inverted trapezoidal feature of being large in the middle and small on both sides. The maximum settlement was approximately located in the middle of the embankment's loading, and the value was positively correlated with the height of the loading. At the foot of the embankment, as it moved away from the foot of the slope, the vertical displacement of the embankment gradually changed from settlement to upward uplift. This is mainly due to the sliding trend of the embankment slope towards the outside caused by loading, and the foot of the embankment slope was subjected to lateral compression. Further analysis showed that in both Condition 1 and Condition 2, there was a significant soil arching effect between the piles, which transferred the overlying load to the pile at the arch foot through the soil arching, thereby improving the bearing capacity of the pile-net composite foundation. In addition, there was relative deformation between the pile and the soil, which was mainly caused by the difference in stiffness. After soil consolidation was completed, the maximum settlement deformation of the embankment in Condition 1 and Condition 2 was 32.1 mm and 18.1 mm, respectively.

Similarly, Figure 18c,d plot the contour maps of the settlement displacement of the pile-net composite foundation along the longitudinal section of the embankment under Condition 3 (PHC pile) and Condition 4 (CFG pile) at the end of soil consolidation, respectively. The figures show the surface settlement curves under different working conditions. From Figure 18c, it can be seen that the settlement curve of the longitudinal section of the embankment was approximately rectangular, indicating that there was little difference in the settlement deformation of the foundation under the same pile-net composite foundation when the loading and the pile length were constant. The settlement mainly depended on geological conditions, and the maximum settlement was located in areas with poor geological conditions. However, the settlement curve of the embankment's longitudinal section in Figure 18d can be divided into two rectangles, with differential settlement occurring at the boundary. This is mainly due to the significant variation in the strata of this section (as shown in Figure 17d), and the length of the CFG pile in the longitudinal section of the embankment had changed, resulting in differences in settlement between the two. In addition, the soil arching effect between piles was more obvious, further indicating the soil reinforcement effect of the pile-net composite foundation. After the completion of soil consolidation, the maximum settlement deformation of the foundation under Condition 3 and Condition 4 was 33.8 mm and 19.8 mm, respectively.

Figure 18e shows the contour map of the settlement displacement of the pile-net composite foundation along the longitudinal section of the embankment under Condition 5 (the transition zone between PHC and CFG piles) at the end of soil consolidation. Similarly, the figure also shows the surface settlement curve under Condition 5.

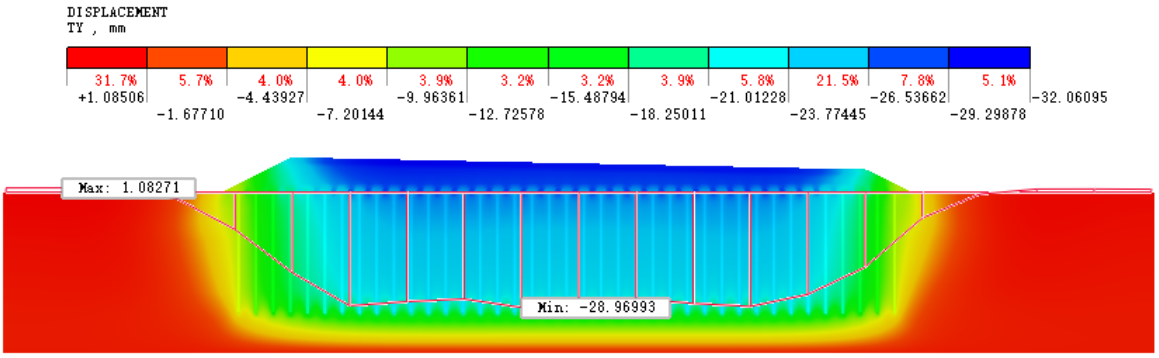

(**a**)

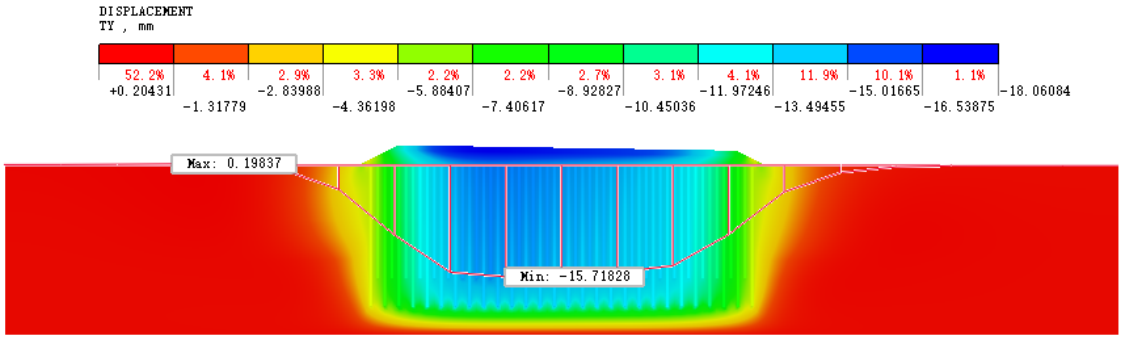

(**b**)

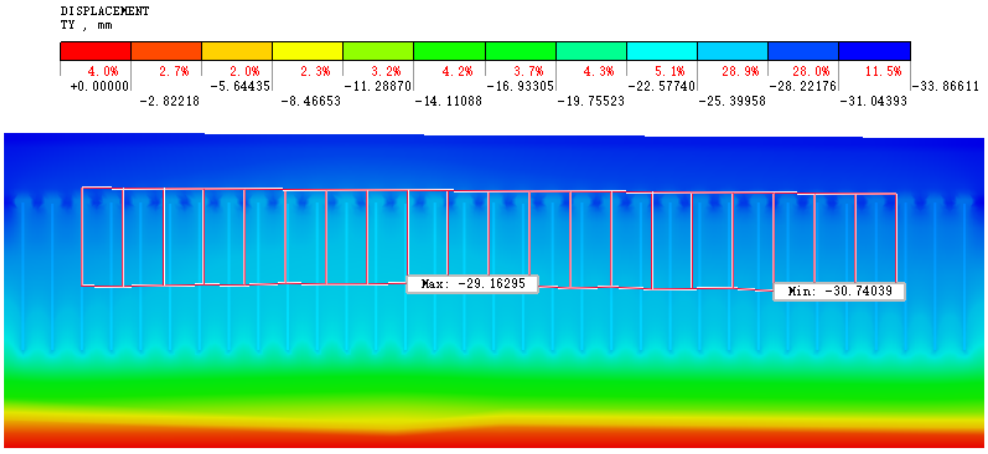

(**c**)

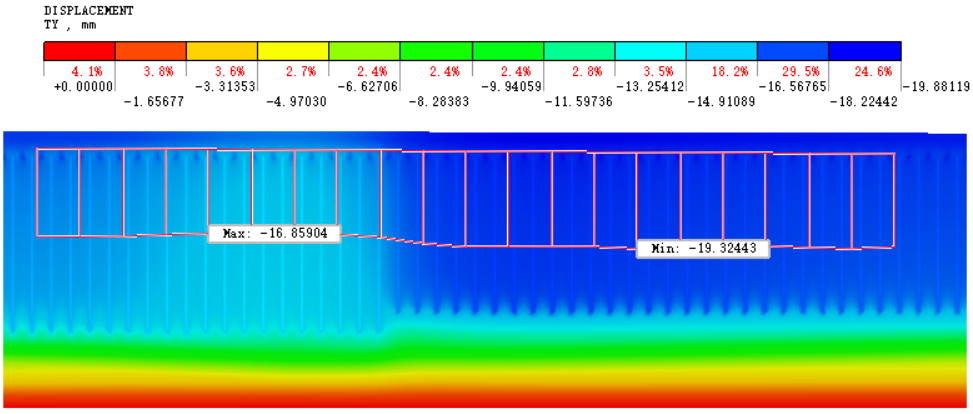

(**d**)

Figure 18. *Cont*.

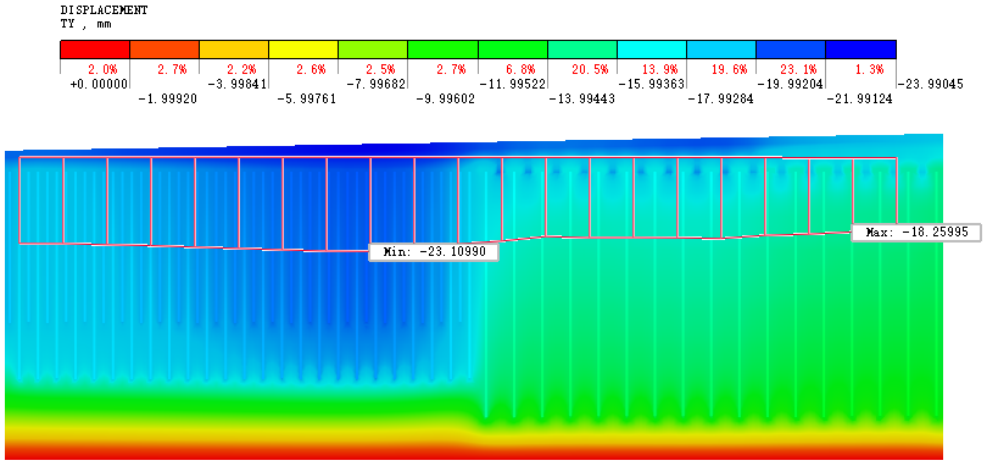

(**e**)

Figure 18. Settlement contour maps and curves of the embankment bottom under different working conditions at the end of soil consolidation: (**a**) Condition 1. (**b**) Condition 2. (**c**) Condition 3. (**d**) Condition 4. (**e**) Condition 5.

From the figure, it can be seen that the settlement curve of the longitudinal section of the embankment can be divided into two rectangles, and there was a significant difference in settlement at the boundary of the two rectangles. This is mainly due to the fact that this section belonged to a transitional zone and two foundation treatment methods, PHC pile and CFG pile, were adopted. The different stiffness of the two types of pile led to the difference in settlement. Further analysis showed that the deformation of soil with the PHC pile was significantly smaller than that with the CFG pile, indicating that the pile-net composite foundation with a higher stiffness had better settlement control. In addition, whether it was the PHC pile or CFG pile, there was a significant soil arching effect between piles, indicating that the pile spacing in this project was relatively reasonable, fully exerting the comprehensive reinforcement effect of a pile-net composite foundation. After soil consolidation was completed, the maximum settlement deformation of the embankment under Condition 5 was located at the boundary between the two types of pile, with a value of 30 mm.

5.3.2. The Effect of the Pile-Net Composite Foundation on Lateral Deformation

In order to analyze the lateral displacement characteristics of the soil at the bottom of the embankment after soil consolidation, the PHC pile-net composite foundation under Condition 1 was taken as an example.

Figure 19 shows the contour map of the lateral displacement of soil along the cross-section of the embankment of the pile-net composite foundation under typical working conditions. The figure also shows the variation curve of the lateral displacement of typical soil with depth. As shown in the figure, the lateral displacement of the deep soil stratum in the middle of the embankment was the smallest, about 2.2 mm, and the lateral displacement gradually decreased with increasing depth. However, the maximum lateral deformation occurred near the foot of the embankment slope, about 5~10 mm.

In addition, the lateral deformation at the foot of embankment decreased first, then increased and then decreased with the depth. The lateral deformation at the foot of the embankment on both sides showed an approximately symmetrical trend with depth. This is mainly because the soil stratum in the loading area was not significantly deformed due to lateral constraints, while there was a free surface near the foot of the embankment. Under the loading effect, stress concentration occurred near the foot of the slope, resulting in a sliding trend of the embankment slope. The lateral deformation of the soil stratum was significantly increased due to lateral compression. When it exceeded a certain depth, the

effect of local stress concentration was weakened, resulting in the lateral displacement gradually decreasing with the increase of depth.

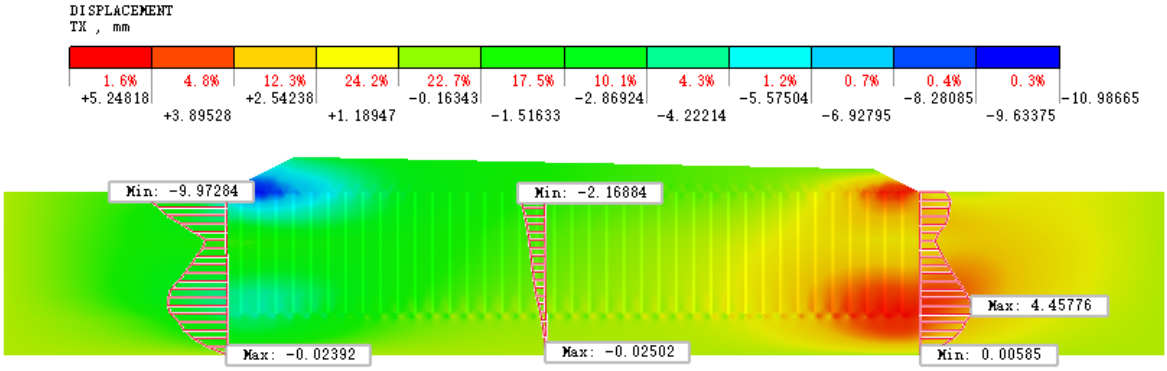

Figure 19. Contour map of the lateral displacement of soil along the cross-section of the embankment under Condition 1 after soil consolidation, and the variation curve of the lateral displacement of soil at typical locations with depth.

5.3.3. The Effect of the Pile-Net Composite Foundation on the Bearing Capacity of Piles

In order to analyze the influence of the pile-net composite foundation on the axial force at the end of soil consolidation, the typical working conditions 1 (PHC pile) and 5 (transition zone between PHC piles and CFG piles) were used as examples for research.

Figure 20a plots the contour map of the axial force of the pile along the cross-section of the embankment under Condition 1 after soil consolidation. As shown in the figure, the axial force near the foot of the embankment on both sides was relatively small, with a value of about 66 kN, while the axial force of the pile located within the range of the top of the slope on both sides was relatively large, with a maximum axial force of 382.3 kN. This is mainly due to the existence of a free surface near the foot of the embankment slope. Under the loading effect, the embankment slope exhibited a sliding trend, causing a certain deflection of the direction of the pile's force in this area. Then, the horizontal force component appeared, which made the piles prone to being damaged by shear and bending moments. However, the vertical axial force value was not significant. In addition, as the depth increased, the axial force of the pile first increased and then decreased. This is mainly due to the fact that soil settlement near the surface was significantly greater than that of the pile in the loading area, and there was a differential settlement between the two. The pile was not only subjected to gravity and the load transmitted by the heaped soil, but also bore the downward pull force (i.e., negative frictional resistance) of the soil. The force on the pile gradually increased with depth. When exceeding a certain depth (the critical depth is called the neutral plane), the settlement of pile was greater than that of surrounding soil, and the pile was subjected to upward frictional resistance. The force on the pile gradually decreased with depth. This was basically consistent with the results of Abushar et al. [45].

Figure 20b shows the axial force diagram of the pile along the longitudinal section of the embankment under Condition 5 after soil consolidation. As shown in the figure, whether it was PHC pile or CFG pile, the axial force of the pile showed a distribution law of first increasing and then decreasing with the increase of depth. The maximum axial force was located in the middle and lower parts of the pile, which was consistent with the above conclusion. In addition, when the loading was constant, the axial force of the PHC pile was relatively small, with a maximum of about 35 kN, while the axial force of the CFG pile could reach a maximum of 560 kN. Further analysis showed that, due to the settlement difference between the two types of piles at the boundary, the friction force was more complex after superposition, resulting in an increase in the axial force of the longer PHC pile and a decrease in the axial force of the shorter CFG pile. When exceeding a certain horizontal range, the influence of the superimposed friction at the boundary on the pile gradually weakened.

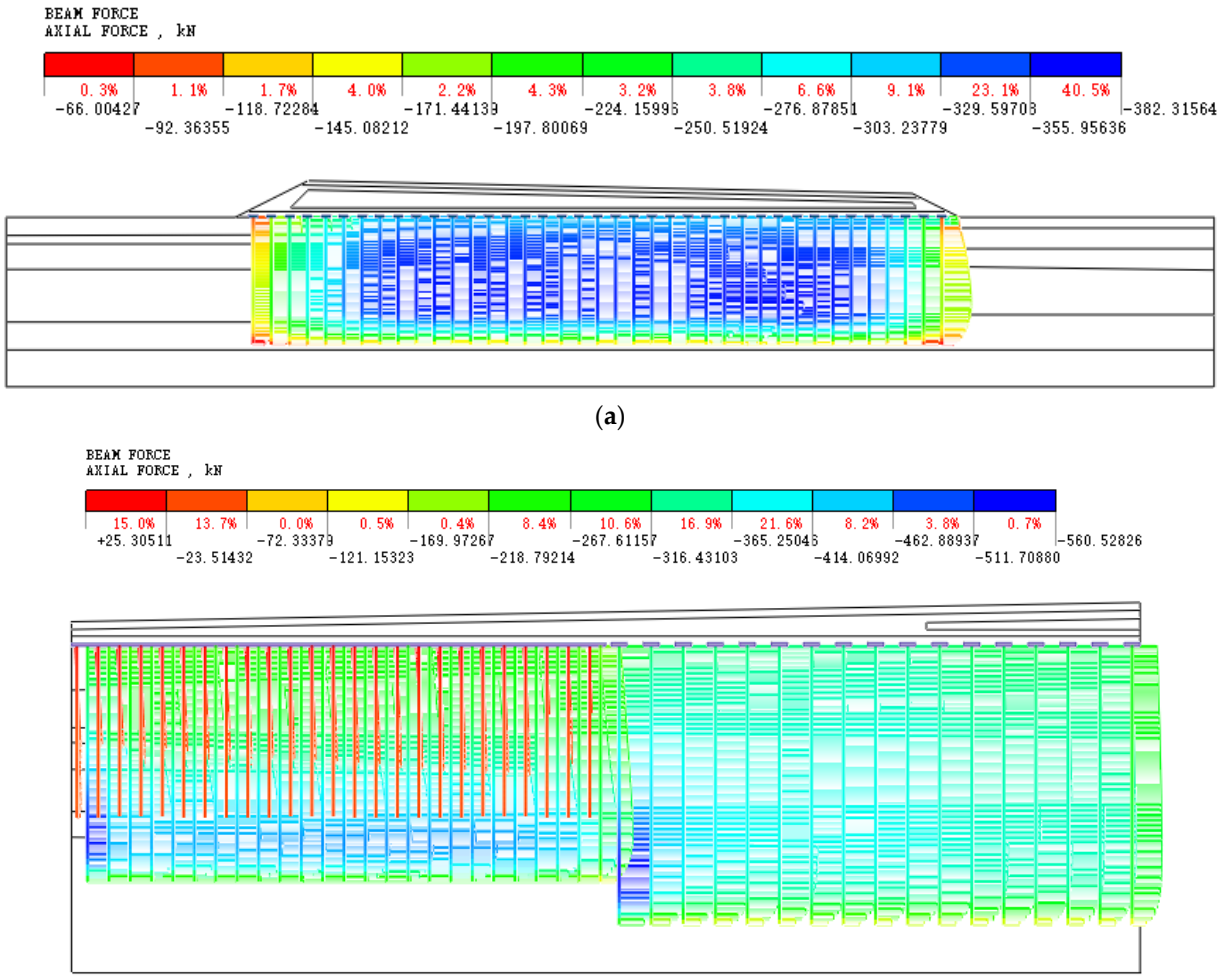

Figure 20. Pile axis diagram under different working conditions after consolidation: (**a**) Condition 1. (**b**) Condition 5.

Similarly, in order to analyze the influence of the pile-net composite foundation on the bending moment of piles at the end of soil consolidation, Figure 21 shows the variation of the bending moment of piles with depth under different working conditions.

Figure 21a,b show the bending moment diagrams of the pile along the cross-section of the embankment under Condition 1 (PHC pile) and Condition 2 (CFG pile) after soil consolidation. As shown in the figure, the piles at the foot of the embankment slopes on both sides were subjected to significant lateral horizontal forces due to loading. Then, there was a sliding trend in the embankment slope, resulting in a large bending moment of the piles in this area. At the same time, the bending moment turns at the soft soil interface. The pile near the middle of the embankment was mainly subjected to a vertical load, and its bending moment was relatively small, generally not exceeding 3 kN·m. After soil consolidation was completed, the maximum bending moment values for Condition 1 and 2 were 21.8 kN·m and 29.5 kN·m, respectively.

Figure 21c,d show the bending moment diagrams along the longitudinal section of the embankment under Condition 3 (PHC pile) and Condition 4 (CFG pile) at the end of soil consolidation. As shown in the figure, the bending moment values are relatively large in areas with significant geological differences and at the foot of the slope, while the bending moment values of the pile are relatively small beyond a certain horizontal distance. After soil consolidation was completed, the maximum bending moment values for Condition 3 and 4 were 28.1 kN·m and 16.6 kN·m, respectively.

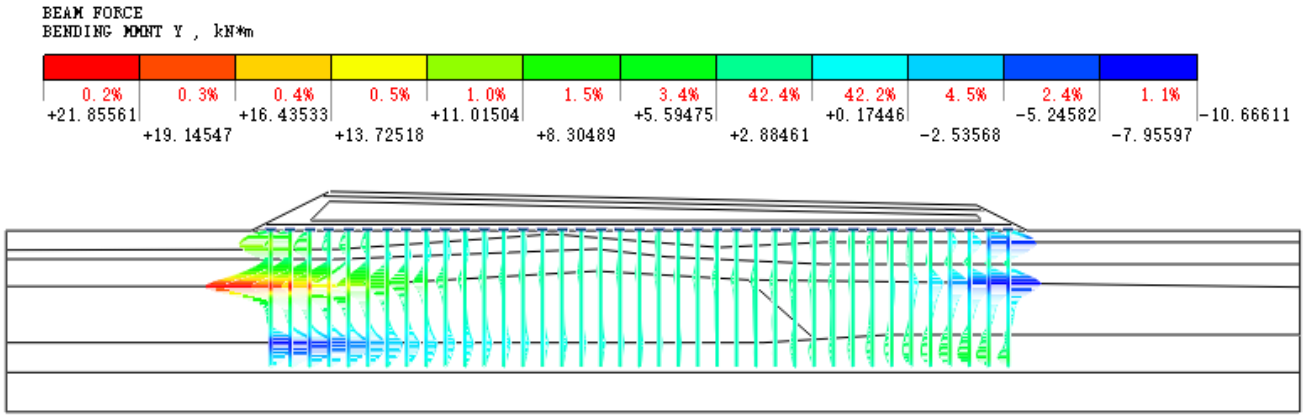

(**a**)

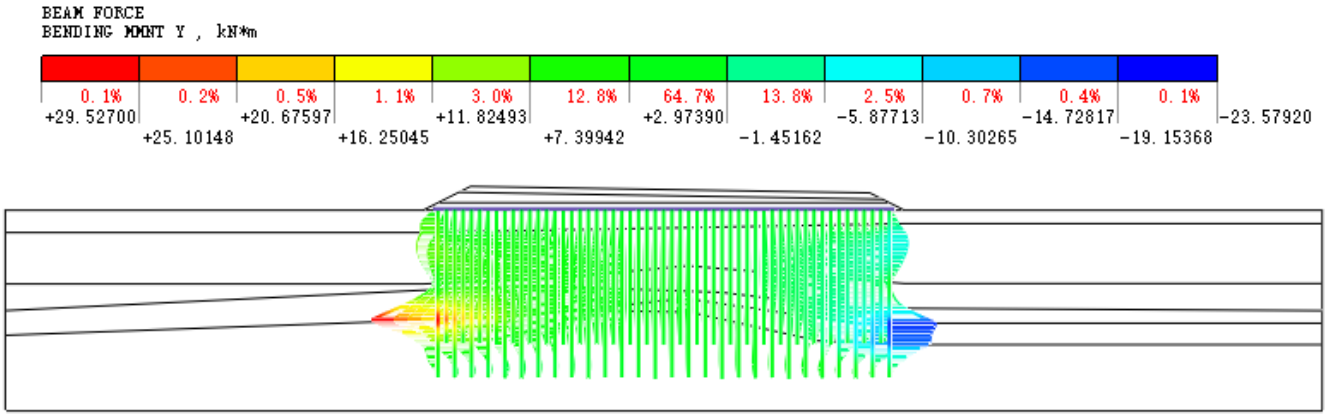

(**b**)

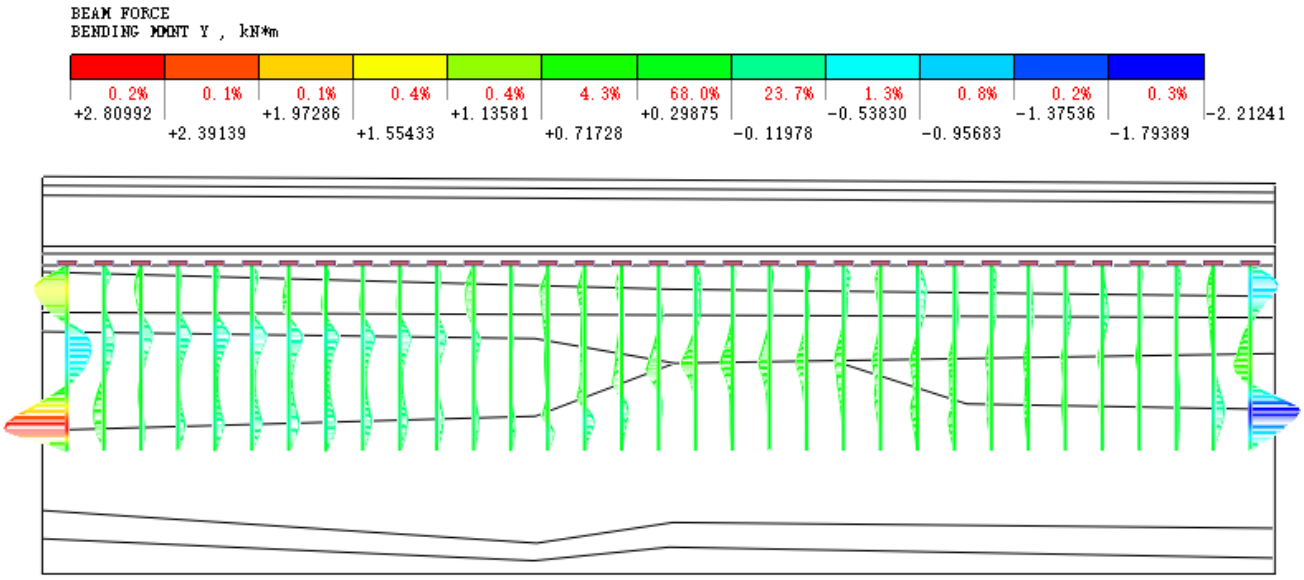

(**c**)

Figure 21. *Cont.*

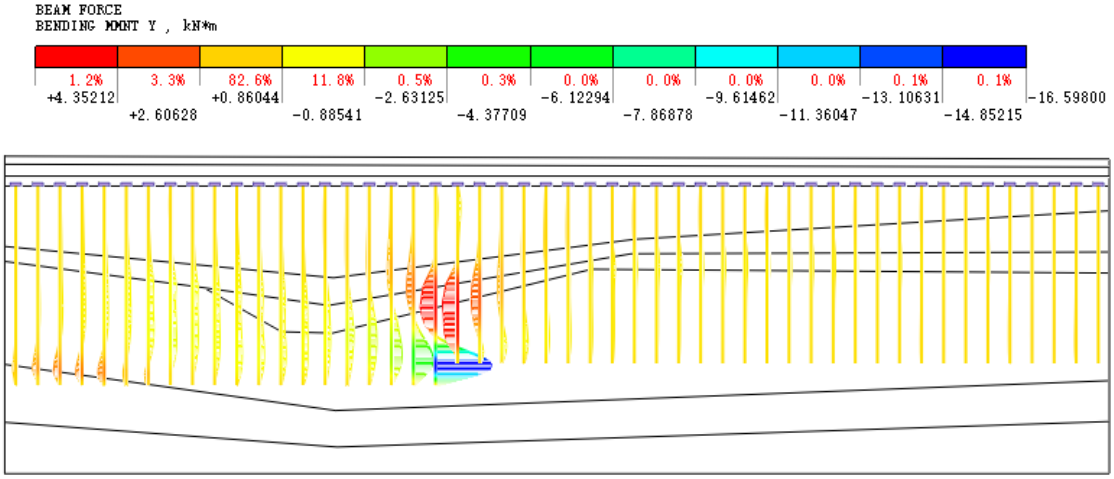

(**d**)

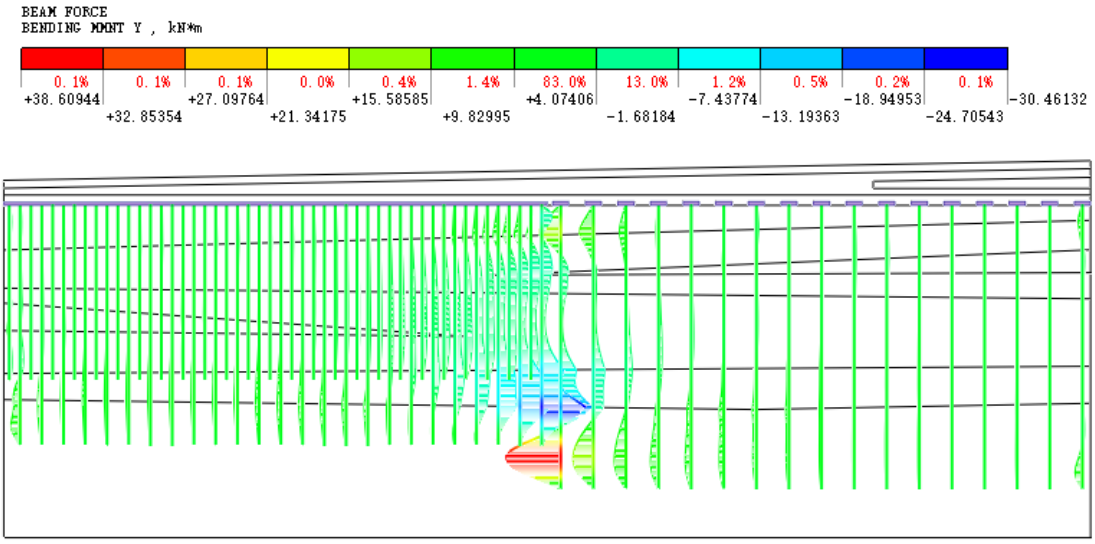

(**e**)

Figure 21. Bending moment diagram of piles under different working conditions at the end of consolidation: (**a**) Condition 1. (**b**) Condition 2. (**c**) Condition 3. (**d**) Condition 4. (**e**) Condition 5.

Figure 21e plots the bending moment diagram of the pile along the longitudinal section of the embankment under Condition 5 after soil consolidation. As shown in the figure, the bending moment at the boundary between the PHC pile and CFG pile was relatively large, reaching up to 38.6 kN·m. However, after exceeding a certain horizontal distance, the bending moment of both types of piles was relatively small, generally not exceeding 2.0 kN·m. Therefore, the maximum bending moment of the pile was mainly located at the foot of the slope or at the boundary of different types of piles, and turned on the interface of the soil strata. The bending moment of the piles in other parts bore less force.

5.4. Comprehensive Evaluation of Settlement Control

Based on the above results, we can obtain the post-construction settlement and the longitudinal uneven settlement ratio (LUSR) of embankments under typical working conditions after soil consolidation. Then, the treatment scheme of the pile-net composite foundation of the motor racing circuit can be evaluated.

Considering that the embankment is filled layer by layer, the total settlement of the embankment can be calculated, but the post-construction settlement is difficult to distinguish. According to reference [46], the post-construction settlement of the embankment is

0.8 percent of the total settlement. In addition, the maximum LUSR of the embankment can be obtained by calculating the section with significant curve changes according to the settlement curve of the embankment (see Figure 18c,d). Based on the calculation results in Section 5.3.1, the embankment settlement and LUSR under typical working conditions after soil consolidation are listed in Table 4. It can be seen from the table that after soil consolidation was completed, the maximum post-construction settlement of the embankment under the most unfavorable conditions of the project was 27 mm, located in the range of pile no. TR1 + 700~TR1 + 800, where the PHC pile-net composite foundation treatment was adopted. The largest LUSR of the embankment was 1.3/4000, located in the range of pile number TR0 + 160~TR0 + 260, which was the transition zone between the PHC pile and CFG pile-net composite foundations. In addition, in terms of pile bearing capacity, combined with the calculation results in Section 5.3.3, it can be seen that when soil consolidation was completed, the maximum axial force values of the PHC pile and CFG pile were 382.3 kN and 560 kN, respectively, which were mainly located in the middle and lower parts of the piles at the top of the embankment slope. The maximum bending moment values were 21.8 kN·m and 38.6 kN·m, respectively, which were mainly located at the foot of the embankment and the boundary between different types of piles.

Table 4. Settlement and LUSR of the embankment under typical working conditions after soil consolidation.

Working Conditions	Pile-Net Composite Foundation	Pile No.	Total Settlement/mm	Post-Construction Settlement /mm	The Longitudinal Uneven Settlement Ratio (LUSR)
Condition 1	PHC pile	TR3 + 260	32.1	25.7	/
Condition 2	CFG pile	TR1 + 440	18.0	14.4	/
Condition 3	PHC pile	TR1 + 700~TR1 + 800	33.8	27.0	0.2/4000
Condition 4	CFG pile	TR3 + 460~TR3 + 560	19.8	15.8	0.55/4000
Condition 5	PHC pile and CFG pile	TR0 + 160~TR0 + 260	24.0	19.2	1.3/4000

It can be concluded that after soil consolidation, the maximum post-construction settlement of the embankment was 27.0 mm < 50.0 mm, and the LUSR of the embankment was 1.3/400 < 3/4000, both of which met the settlement control standards of the embankment. Moreover, the axial force and bending moment of the pile were within the range of their compressive and bending strength, indicating that the pile-net composite foundation treatment scheme adopted in this project was feasible. It provides a guarantee of the safe construction and operation of the project.

6. Discussion

Through field tests, the back analysis of stratum parameters and pile moduli, and the numerical simulation of mechanical characteristics of pile-net composite foundations under five typical working conditions considering the construction process, the embankment settlement and differential settlement after soil consolidation in the motor racing circuit were deeply studied, and the following understandings could be obtained:

In terms of settlement and lateral deformation, for soft soil strata, whether the PHC pile or CFG pile-net composite foundation treatment was adopted, the settlement of the soil between piles was significantly greater than the settlement of the pile head. Namely, in this project, the settlement of soil between piles was 2.7 to 3.7 times that of adjacent pile head, and the worse the strata conditions, the greater the difference between the settlement of soil between piles and the pile head.

When it comes to the pile-net composite foundation treatment of weak soil embankments, a rigid pile, such as PHC pile or CFG pile, is commonly used. For the areas that do not meet the requirements, the method of high pressure grouting reinforcement near the pile body is often adopted. Under the process of high pressure grouting, although a reinforcement effect can be obtained, some failure phenomena such as deformation, tilt, and even damage to the pile body often occur. In order to solve this problem effectively,

this paper puts forward a safe and effective remedy, which is adding PHC pile and CFG pile, and using a cement–soil mixing pile between the rigid piles. This method makes full use of the squeezing effect, which can significantly reduce post-construction settlement and avoid its influence on the adjacent pile. Compared with the traditional remedial method, the proposed method in this paper has the advantages of faster construction speed and a better effect, and has been successfully applied in practical engineering applications.

In terms of pile–soil interaction parameters, due to the deep soft soil in the project area, in order to fully utilize the bearing capacity of the pile-net composite foundation, the piles were arranged reasonably to ensure that the overall stress on the pile and soil was uniform. A pile-net composite foundation mainly bears vertical loading. So, the parameters that have a significant impact on the settlement and deformation control of the embankment are the elastic modulus of the pile and the deformation modulus of the soil strata. Considering that soil strata in the test sections mainly include 2-2 silty clay, 2a clay, 4 silty clay, and 6-1 silt, it is necessary to invert the deformation modulus of the above soil strata, as well as elastic modulus of the PHC piles and CFG piles. Based on the laboratory test results, the relationship between the compressive modulus and deformation modulus of the strata, construction disturbance, the distribution range of the deformation modulus of the strata, and the elastic modulus of the CFG and PHC piles can be preliminarily determined. Then, based on the measured data, the above parameters can be inverted and analyzed to obtain more reasonable pile–soil interaction parameters. Research has shown that the soil deformation modulus and pile modulus have a significant impact on embankment settlement. The larger the values of both the soil deformation modulus and pile modulus, the smaller the embankment settlement, which is basically consistent with the actual situation.

In terms of pile bearing capacity, regardless of whether the PHC pile- or CFG pile-net composite foundation was used for the deep embankment treatment, the axial force of the piles increased first and then decreased with depth, and the maximum axial force was located in the middle and lower part of the piles. This is mainly because the soil settlement near the surface was obviously greater than the settlement of piles in the loading area, and there was differential settlement between the two. The downward pull (i.e., negative friction resistance) transmitted by gravity and heaped soil made the force of pile gradually increase with depth. When the depth exceeded a certain level, the settlement of the pile was greater than that of the surrounding soil, and the pile was subjected to upward friction resistance, and the force of the pile gradually decreased with depth. In addition, the maximum bending moment was located at the foot of the slope and the boundary between different types of piles, which was smaller in the middle of the embankment, and the bending moment turned at the interface of soft soil. This is mainly due to the sliding trend of the embankment at the foot of the slope, resulting in a larger bending moment of the pile, while the pile near the middle of the embankment was mainly subjected to a vertical load, and its bending moment was relatively small. Moreover, when the pile-net composite foundation was adopted for embankment treatment, the axial force and bending moment of the pile were generally not large. The maximum axial force of the project was 560 kN, and the maximum bending moment was 38.6 kN·m. The axial force and bending moment were both within the range of the compressive and bending strength of the pile.

Further analysis showed that no matter whether PHC pile or CFG pile, there was an obvious soil arching effect between piles, and the soil arching effect was conducive to enhancing the reinforcement effect of composite foundation. In practical engineering, the pile spacing should be rationally arranged. In this project, when the pile spacing was 3–4 times the pile diameter, the soil arching effect of the pile-net composite foundation was the best. It is worth mentioning that the pore water pressure dissipated slowly due to the short field test time, the interference of the construction load, and the heaped soil. After the completion of the field test, there was still nearly 20 kPa of pore water pressure, which failed to fully reflect the settlement characteristics. Therefore, there might be some

differences between the calculated results and the actual ones, which could be further discussed in the future.

7. Conclusions

Taking the Wuhan intelligent connected motor racing circuit as our setting, a method of combining field tests with numerical simulation was proposed to identify, treat, and evaluate embankment settlement and differential settlement under typical working conditions, such as deep soft soil sections, sudden geological changes, and transition sections, with different pile types. The main conclusions are as follows:

(1) Field tests showed that for medium or high filling areas, the maximum settlement of the pile head and soil between piles was 13.6 mm and 50.41 mm, respectively, and the settlement of soil between piles was 3.5~3.7 times that of adjacent pile heads. For low filling areas, the maximum settlement of the pile head and soil between piles was 13.34 mm and 39.65 mm, respectively. The cumulative settlement value of the pile head and soil between piles increased in a hyperbolic form. The lateral displacement direction of the soil strata in the loading area was spread outward from the loading center, and the lateral displacement did not exceed 1.5 mm.

(2) Based on field test data, the GA-BP method, combining the uniform design method, was used to carry out back analysis on the mechanical parameters of the soil strata and pile modulus. The results showed that the settlement calculation values were basically consistent with the measured ones, with an error of no more than 10%, indicating good inversion accuracy. In addition, after soil consolidation, the predicted maximum settlement values of the PHC pile and CFG pile in the two pile test sections were about 70 mm and 59 mm, respectively. By adding PHC piles, CFG piles, and reinforcing cement–soil mixing piles between the piles, the maximum settlements were 21.01 mm and 15.88 mm, respectively, meeting the settlement control requirements.

(3) By selecting five typical working conditions, a numerical analysis was conducted on the settlement and pile bearing capacity of the embankment in the engineering area. The calculation showed that after the soil consolidation was completed, the maximum settlement of the embankment was 27.0 mm, and the maximum LUSR of the embankment was 1.3/4000. The maximum lateral displacement in the middle of the embankment is about 2.2 mm. The maximum axial forces of the PHC piles and CFG piles were 382.3 kN and 560 kN, respectively, and the maximum bending moments were 21.8 kN·m and 38.6 kN·m. The axial forces and bending moments of the piles were within their compressive and flexural strength ranges. It can be concluded that the pile-net composite foundation treatment methods adopted in this project were feasible, and the embankment settlement and differential settlement were controllable, which can meet safety and operational requirements.

However, the current research on pile-net composite foundations in soft soil areas mainly focuses on the bearing characteristics and deformation control effects of a certain soil stratum. The theory, laboratory equipment, and field tests for predicting embankment settlement in the different transition zones of pile-net composite foundations and multiple spatial variation zones of a soft soil stratum are not yet mature, and further study is needed.

Author Contributions: X.W.: methodology, investigation, and supervision; Q.P.: methodology, data curation, validation, writing, and funding acquisition. All authors have read and agreed to the published version of the manuscript.

Funding: This research was funded by the National Science Foundation of China (No. 51609018).

Data Availability Statement: The data used to support the findings of this study are included in the article.

Conflicts of Interest: Author Xiaonan Wang was employed by the company Wuhan Urban Construction Investment Development Group Co., Ltd. and Author Qitao Pei was employed by the company Wuhan Municipal Engineering Design & Research Institute Co., Ltd. The companies were

not involved in the study design, collection, analysis, interpretation of data, the writing of this article or the decision to submit it for publication.

References

1. Yin, J.H.; Feng, W.Q. A new simplified method and its verification for calculation of consolidation settlement of a clayey soil with creep. *Can. Geotech. J.* **2017**, *54*, 333–347. [CrossRef]
2. Zhu, H.H.; Zhang, C.C.; Mei, G.X.; Shi, B.; Gao, L. Prediction of one-dimensional compression behavior of Nansha clay using fractional derivatives. *Mar. Georesources Geotechnol.* **2017**, *35*, 688–697. [CrossRef]
3. Zhang, S.M.; Jian, G.L.; Liao, Y.L. Effect of the strengthening area and the slope rate on bearing and deforming behaviors of CFG pile-geogrid composite foundations. *Chin. J. Rock Mech. Eng.* **2019**, *38*, 192–202.
4. Zheng, G.; Zhao, J.P.; Zhou, H.Z. State-of-the-art review for techniques on ground improvement of highway and railway. *Chin. J. Ground Improv.* **2021**, *3*, 91–99. (In Chinese)
5. Wu, P.C.; Yin, J.H.; Feng, W.Q.; Chen, W.B. Experimental study on geosynthetic-reinforced sand fill over marine clay with or without deep cement mixed soil columns under different loadings. *Undergr. Space* **2019**, *4*, 340–347. [CrossRef]
6. Reshma, B.; Rajagopal, K.; Viswanadham, B.V.S. Centrifuge model studies on the settlement response of geosynthetic piled embankments. *Geosynth. Int.* **2020**, *27*, 170–181. [CrossRef]
7. Wu, P.C.; Feng, W.Q.; Yin, J.H. Numerical study of creep effects on settlements and load transfer mechanisms of soft soil improved by deep cement mixed soil columns under embankment load. *Geotext. Geomembr.* **2020**, *48*, 331–348. [CrossRef]
8. Esen, A.F.; Woodward, P.K.; Laghrouche, O.; Čebašek, T.M.; Brennan, A.J.; Robinson, S.; Connolly, D.P. Full-scale laboratory testing of a geosynthetically reinforced soil railway structure. *Transp. Geotech.* **2021**, *28*, 100526. [CrossRef]
9. Arulrajah, A.; Abdullah, A.; Bo, M.W.; Bouazza, A. Ground improvement techniques for railway embankments. *Proc. Inst. Civ. Eng. Ground Improv.* **2009**, *162*, 3–14. [CrossRef]
10. Terzaghi, K. *Theoretical Soil Mechanics*; Wiley: New York, NY, USA, 1943.
11. Low, B.K.; Tang, S.K.; Choa, V. Arching in piled embankments. *J. Geotech. Eng.* **1994**, *120*, 1917–1938. [CrossRef]
12. Giroud, J.P.; Bonaparte, R.; Beech, J.F.; Gross, B.A. Design of soil layer-geosynthetic systems overlying voids. *Geotext. Geomembr.* **1990**, *9*, 11–50. [CrossRef]
13. Hewlett, W.J.; Randolph, M.F. Analysis of piled embankments. *Ground Eng.* **1988**, *21*, 12–18.
14. Chen, Y.M.; Cao, W.P.; Chen, R.P. An experimental investigation of soil arching within basal reinforced and unreinforced piled embankments. *Geotext. Geomembr.* **2008**, *26*, 164–174.
15. Castro, J.; Sagaseta, C. Consolidation and deformation around stone columns: Numerical evaluation of analytical solutions. *Comput. Geotech.* **2011**, *38*, 354–362. [CrossRef]
16. Liu, F.; Zhang, J.J. Centrifuge test on deformation characteristics of pile-geogrid composite foundation in soft soil under slope. *Chin. J. Rock Mech. Eng.* **2018**, *37*, 209–219.
17. Blanc, M.; Rault, G.; Thorel, L.; Almeida, M. Centrifuge investigation of load transfer mechanisms in a granular mattress above a rigid inclusions network. *Geotext. Geomembr.* **2013**, *36*, 92–105. [CrossRef]
18. Fagundes, D.F.; Almeida, M.S.; Thorel, L.; Blanc, M. Load transfer mechanism and deformation of reinforced piled embankments. *Geotext. Geomembr.* **2017**, *45*, 1–10. [CrossRef]
19. Girout, R.; Blanc, M.; Thorel, L.; Dias, D. Geosynthetic reinforcement of pile-supported embankments. *Geosynth. Int.* **2018**, *25*, 37–49. [CrossRef]
20. Das, A.K.; Deb, K. Experimental and 3D numerical study on time-dependent behavior of stone column–supported embankments. *Int. J. Geomech.* **2018**, *18*, 04018011. [CrossRef]
21. Liu, J.W.L.; Zhang, Z.M.; Zhao, Y.B.; Lin, C.G. Statistical research on performance of prestressed concrete pipe piles. In Proceedings of the 2011 International Conference on Electric Technology and Civil Engineering (ICETCE), Lushan, China, 22–24 April 2011; pp. 711–714.
22. Oh, Y.I.; Shin, E. C Reinforcement and arching effect of geogrid-reinforced and pile-supported embankment on marine soft ground. *Mar. Georesources Geotechnol.* **2007**, *25*, 97–118. [CrossRef]
23. Zhang, C.; Jiang, G.; Liu, X.; Buzzi, O. Arching in geogrid-reinforced pile-supported embankments over silty clay of medium compressibility: Field data and analytical solution. *Comput. Geotech.* **2016**, *77*, 11–25. [CrossRef]
24. Yang, M.; Liu, S. Field tests and finite element modeling of a prestressed concrete pipe pile-composite foundation. *KSCE J. Civ. Eng.* **2015**, *19*, 2067–2074. [CrossRef]
25. Zhang, S.; Tang, C. Subgrade Settlement of High Speed Railway in Seasonal Frozen Soil Area. *J. Northeast. Univ. (Nat. Sci.)* **2013**, *34*, 1202–1205.
26. Zhang, F.; Liu, Y.; Xu, Z.Y.; Li, Z.Y. Factors influencing subgrade post-construction settlement of CFG pile composite foundation in Wuhan-Guangzhou high-speed railway. *J. Southwest Jiaotong Univ.* **2015**, *50*, 783–788.
27. Yoo, C. Settlement behavior of embankment on geosynthetic-encased stone column installed soft ground—A numerical investigation. *Geotext. Geomembr.* **2015**, *43*, 484–492. [CrossRef]
28. Zhao, L.S.; Zhou, W.H.; Fatahi, B.; Li, X.B.; Yuen, K.V. A dual beam model for geosynthetic-reinforced granular fill on an elastic foundation. *Appl. Math. Model.* **2016**, *40*, 9254–9268. [CrossRef]

29. Jamsawang, P.; Yoobanpot, N.; Thanasisathit, N.; Voottipruex, P.; Jongpradist, P. Three-dimensional numerical analysis of a DCM column-supported highway embankment. *Comput. Geotech.* **2016**, *72*, 42–56. [CrossRef]
30. Nunez, M.A.; Briançon, L.; Dias, D. Analyses of a pile-supported embankment over soft clay: Full-scale experiment, analytical and numerical approaches. *Eng. Geol.* **2013**, *153*, 53–67. [CrossRef]
31. Hájek, V.; Mašín, D.; Boháč, J. Capability of constitutive models to simulate soils with different OCR using a single set of parameters. *Comput. Geotech.* **2009**, *36*, 655–664. [CrossRef]
32. Yan, W.M.; Li, X.S. Mechanical response of a medium-fine-grained decomposed granite in Hong Kong. *Eng. Geol.* **2012**, *129*, 1–8. [CrossRef]
33. Abad, S.A.N.K.; Tugrul, A.; Gokceoglu, C.; Armaghani, D.J. Characteristics of weathering zones of granitic rocks in Malaysia for geotechnical engineering design. *Eng. Geol.* **2016**, *200*, 94–103. [CrossRef]
34. Deb, K. A mathematical model to study the soil arching effect in stone column-supported embankment resting on soft foundation soil. *Appl. Math. Model.* **2010**, *34*, 3871–3883. [CrossRef]
35. Zhuang, Y.; Wang, K. Finite element analysis on the dynamic behavior of soil arching effect in piled embankment. *Transp. Geotech.* **2018**, *14*, 8–21. [CrossRef]
36. Zhao, L.S.; Zhou, W.H.; Geng, X.; Yuen, K.V.; Fatahi, B. A closed-form solution for column-supported embankments with geosynthetic reinforcement. *Geotext. Geomembr.* **2019**, *47*, 389–401. [CrossRef]
37. Chen, R.P.; Zhou, W.H.; Chen, Y.M. Influences of soil consolidation and pile load on the development of negative skin friction of a pile. *Comput. Geotech.* **2009**, *36*, 1265–1271. [CrossRef]
38. Yu, J.; Cai, Y.; Qi, Z.; Guan, Y.; Liu, S.; Tu, B. Analytical analysis and field test investigation of consolidation for CCSG pile composite foundation in soft clay. *J. Appl. Math.* **2013**, *2013*, 795962. [CrossRef]
39. Filz, G.M.; Sloan, J.A.; McGuire, M.P.; Smith, M.; Collin, J. Settlement and vertical load transfer in column-supported embankments. *J. Geotech. Geoenvironmental Eng.* **2019**, *145*, 04019083. [CrossRef]
40. Luo, Q.; Lu, Q.Y. Settlement calculation of rigid pile composite foundation considering pile-soil relative slip under embankment load. *China J. Highw. Transp.* **2018**, *31*, 20–30. (In Chinese)
41. Institute of Rock and Soil Mechanics, Chinese Academy of Sciences. *Monitoring Project for Closed Test Field of Wuhan New Energy and Intelligent Connected Motor-Racing Circuit*; Institute of Rock and Soil Mechanics, Chinese Academy of Sciences: Wuhan, China, 2021. (In Chinese)
42. Wang, H.T.; Tu, B.X.; Su, P.; Gu, X.K. *Numerical Simulation Technology and Engineering Applications of MIDAS GTS NX*; Dalian University of Technology Press: Dalian, China, 2020. (In Chinese)
43. Pei, Q.T.; Li, H.B.; Liu, Y.Q.; Song, Q.J.; Li, N.N. Two-stage back analysis of initial geostress field of dam areas under complex geological conditions. *Chin. J. Rock Mech. Eng.* **2014**, *33*, 2779–2785. (In Chinese)
44. Chen, Z.Y. *Theory Methods and Programs of Soil Slope Stability Analysis*; China Water & Power Press: Beijing, China, 2003. (In Chinese)
45. Abusharar, S.W.; Zheng, J.J.; Chen, B.G. Finite element modeling of the consolidation behavior of multi-column supported road embankment. *Comput. Geotech.* **2009**, *36*, 676–685. [CrossRef]
46. *JTG/T D31-02-2013*; Technical Guidelines for Design and Construction of Highway Embankment on Soft Ground. Chinese Standard: Beijing, China, 2013. (In Chinese)